Research Square

Preprints are preliminary reports that have not undergone peer review.
They should not be considered conclusive, used to inform clinical practice,
or referenced by the media as validated information.

Bioproduction of Neospora caninum: a proof-of-concept towards a scalable serum-free process

Zineb Lakhrif
Université de Tours, INRAE, ISP
Nathalie Moiré
INRAE, Université de Tours, ISP
Audrey Munos-Guillon
BioCube Institute, Groupe IMT
Anne di Tommaso
Université de Tours, INRAE, ISP
Céline Ducournau
Université de Tours, INRAE, ISP
Isabelle Dimier-Poisson
Université de Tours, INRAE, ISP
Cyril Poupet
cyril.poupet@univ-tours.fr

Université de Tours, INRAE, ISP

Research Article

Keywords: Neospora caninum, CHO-K1, serum-free, bioproduction, USP

Posted Date: September 14th, 2026

DOI: https://doi.org/10.21203/rs.3.rs-11006577/v1

License: This work is licensed under a Creative Commons Attribution 4.0 International License.
Read Full License

Additional Declarations: No competing interests reported.

Bioproduction of *Neospora caninum*: a proof-of-concept towards a scalable serum-free process

Authors:

Zineb Lakhrif[1], Nathalie Moiré[2], Audrey Munos-Guillon[3,4], Anne di Tommaso[1], Céline Ducournau[1], Isabelle Dimier Poisson[1], Cyril Poupet[1*]

Affiliations:

[1] Université de Tours, INRAE, ISP, 37380 Nouzilly, France.

[2] INRAE, Université de Tours, ISP, 37380 Nouzilly, France

[3] BioCube Institute, Groupe IMT, Tours, France

[4] LONZA SA, Visp, Switzerland

*** Corresponding author:**

cyril.poupet@univ-tours.fr

ORCID:

Anne di Tommaso: 0000-0002-4826-0333

Céline Ducournau: 0000-0002-0920-2392

Cyril Poupet : 0000-0001-9343-4390

Isabelle Dimier Poisson: 0000-0001-8917-4493

Nathalie Moiré: 0000-0001-9171-5711

Zineb Lahkrif: 0000-0001-9010-8493

Abstract

Neospora caninum is emerging as a promising oncolytic protozoan for cancer immunotherapy. However, large-scale production of tachyzoites remains constrained by a culture system dependent on animal-derived serum and primary-like host cells, limiting standardisation, regulatory compliance, and scalability. Moreover, bioproduction processes for obligate intracellular protozoa are scarce and largely restricted to *Plasmodium* and *Leishmania*. Developing scalable manufacturing strategies for *N. caninum* is therefore a critical bottleneck for clinical translation.

Building on a prior regulatory analysis, which emphasised early integration of classification, quality, and manufacturing constraints, we evaluated industrially relevant mammalian cell lines and serum-reduced or serum-free conditions for protozoa production. BHK-21 and CHO-K1 cells were selected to balance physiological relevance and industrial scalability.

Cells were cultured in defined media and infected with *N. caninum* at varying multiplicities of infection (MOI). Protozoa yield, host cell growth, and glucose/lactate dynamics were monitored to assess production performance and host–protozoa metabolic interactions.

Both cell lines supported protozoa multiplication under serum-free conditions, with a better yield with CHO-K1 than BHK-21 in our experimental conditions. In CHO-K1, production was strongly influenced by medium composition and MOI, with Advanced DMEM/F-12 yielding the highest protozoa output and stable metabolic profiles, while with other media, infection increased glucose consumption.

These findings demonstrate the feasibility of serum-free *N. caninum* production using industrial cell lines (CHO-K1) and identify Advanced DMEM/F-12 as a promising medium for scalable, standardised, and GMP-compatible manufacturing.

Key Points

- CHO-K1 and BHK-21 cells support serum-free *N. caninum* growth
- Advanced DMEM/F-12 maximises protozoa yield and metabolic stability
- Host cell metabolic state critically influences protozoa bioproduction

Key words

Neospora caninum, CHO-K1, serum-free, bioproduction, USP

1 Introduction

Cancer immunotherapy is redefining clinical oncology by recruiting the immune system of patients against tumours. Beyond new immunotherapeutics, oncolytic microorganisms such as viruses and bacteria have been developed. *Mycobacterium bovis* Bacillus Calmette-Guerin (BCG) was the first Food and Drug Administration (FDA) approved oncolytic bacterium (Sfakianos et al. 2021), and recombinant HSV-1 was the first approved oncolytic virus (Pol et al. 2016). Intracellular protozoa have demonstrated the potential to stimulate immune responses against tumours. Among these protozoa, apicomplexans, such as *Toxoplasma* and *Leishmania,* have gained significant attention for their potential anticancer effects (Vuscan et al. 2025). Another protozoan, *N. caninum,* has shown potent oncolytic effects against several tumours in animal models (Lantier et al. 2020; Li et al. 2022; Battistoni et al. 2023). Very strong tumour growth inhibition has been observed in murine models of thymic lymphoma, lung metastasis model of B16F10 melanoma and human Merkel Cell carcinoma following intratumoral or remote injection of this protozoan (Lantier et al. 2020; Battistoni et al. 2023). Therefore, its use for the treatment of cancer requires the development of an optimised *in vitro* production process. Currently, the bioproduction of protozoa for clinical applications is very poorly documented and limited to *Plasmodium falciparum* (Dalton et al. 2012; Pawliw et al. 2018).

N. caninum and *Toxoplasma gondii* are closely related members of the phylum Apicomplexa. Due to their phylogenetic proximity and similar morphology, *N. caninum* was long misidentified as *T. gondii* until its taxonomic reclassification in 1988. Even today, given the limited literature on *N. caninum*, many studies continue to rely on data obtained from *T. gondii*. This can be explained by the zoonotic nature of *T. gondii* and its pathogenicity to humans (Dubey et al. 2007; Reid et al. 2012).

N. caninum, like *T. gondii,* is an obligate intracellular protozoan that cannot be produced without a producer cell. Currently, large-scale production of *N. caninum* is performed using DMEM high glucose in 175 cm^2 flasks with limited scalability. Production also requires a 1 to 5 % foetal bovine serum (FBS) supplementation for the cell culture. *N. caninum* is lab-produced on adherent cell lines like HFF, Vero, MDCK, MDBK, and MARC-145. The survival and replication of intracellular pathogens rely in part on host resources. Both *N. caninum* and *T. gondii* have been shown to scavenge metabolites from their host cell (Nolan et al. 2015), but data on *N. caninum* are scarce in the literature and most publications concern *T. gondii*. Several studies were able to delineate the minimal set of substrates required for *T. gondii* survival and proliferation in *in vitro* culture. A method to identify an *in silico* minimal medium (IMM analysis) revealed 25 substrates required to

fulfil all metabolic needs (Tymoshenko et al. 2015; Chiappino-Pepe et al. 2017; Krishnan et al. 2020). They also classified groups of metabolites that serve as carbon, nitrogen, and sulphur sources needed for *T. gondii* growth and survival. Based on the *T. gondii* data, optimisation and scaling up of the *N. caninum* production process are required for future market release.

The translation of oncolytic protozoa from the laboratory bench to their clinical use is subject to specific regulations and must also meet several well-defined criteria for selectivity, potency, stability, identity, and product characterisation (Guerriaud et al. 2024).

An ideal bioprocess for producing biologics uses a suspension cell line to facilitate scalability and chemically defined, animal component-free cell culture media to avoid challenges concerning lot-to-lot variation, animal welfare, supply, cost, and potential regulatory restrictions in the future.

A series of unit operations ranging from upstream processing to the final sterile filtration, including the analytical methods for process monitoring and control, is required for manufacturing. However, there are still unmet challenges to be overcome in product generation, purification and final characterisation when moving from product development toward product in the clinic.

The removal of serum from the medium is highly recommended to reduce the risk of contamination, costs and to simplify downstream processes (European Medicines Agency 2013). Moreover, animal-component-free media (ACFM) may be preferred to simplify future potential regulatory restrictions concerning animal welfare and animal-derived products.

Scaling up adherent cell culture with intracellular protozoan for mass production involves many challenges and bottlenecks. Attachment-dependent culture is restricted by growth surface area, and bioprocesses of adherent cells involve additional steps, including cell detachment required for subsequent passaging and amplification. However, the adaptation of cells to grow in suspension is also a time-consuming and gradual but necessary process to generate high-yielding cell lines. Moreover, changes in cell surface molecules during adaptation to suspension growth may lead to reduced cell infection by the protozoa, as described for viruses (Dill et al. 2021). Use of microcarriers, macrocarriers and disposable fixed-bed bioreactors limits these issues and increases the surface area available to grow adherent cells in a scalable and efficient way.

The characteristics of these protozoa add to the difficulty of scalable purification for clinical administration. For example, their large size (around 5 µm long) prevents a final sterile filtration

step, requiring aseptic processing conditions to be maintained throughout the entire production process. Furthermore, the protozoan must maintain its infectivity across the entire process.

The present study aimed to establish laboratory-scale upstream process (USP) production and characterisation conditions for *N. caninum* to advance toward clinical-grade production. We compared 2 cell lines (BHK-21 and CHO-K1) usually used to produce biotherapeutics, such as oncolytic viruses or monoclonal antibodies (Moleirinho et al. 2019). We also aimed to set up a process completely devoid of FBS for both steps of culture (cells alone and cells with protozoa).

2 Materials and methods

2.1 Cell lines

All cell cultures were maintained at 37 °C in a humidified atmosphere containing 5 % CO_2. All culture media and supplements were provided by Gibco (Thermo Fisher, Grand Island, USA).

DMEM high glucose (4.5 g/L), DMEM/F-12 or Advanced DMEM/F-12 were supplemented with 1 % GlutaMAX™. For protozoa culture,10 mM HEPES and different percentages of FBS (Biosera, Cholet, France) were used. One percent of Insulin-Transferrin-Selenium (ITS, Gibco) complement was also used to replace FBS.

All cell lines were obtained from ATCC: CHO-K1 cells (Chinese Hamster Ovary, ATCC® CCL-61 ™), BHK-21 [C-13] (ATCC® CCL-10 ™) cells and HFF (ATCC®CRL-1634 ™) cells were either maintained in DMEM high glucose 10 % FBS or adapted to low- or no-serum culture. Adaptation was performed stepwise, and for the condition without serum, BHK-21 cells were used after 4 passages without serum.

2.2 *Neospora caninum* culture

N. caninum NC1 wild-type strain was obtained from ATCC (ATCC®-50977 ™).

Protozoa were maintained in Human Foreskin Fibroblast (HFF) cell culture as previously described (Débare et al. 2021). Tachyzoites of *N. caninum* NC1 were cultured on HFF monolayers maintained in DMEM High glucose containing 1 % FBS, 10 mM HEPES and 1 % GlutaMAX™. Tachyzoites were recovered when complete lysis of the cells was achieved and used for infection experiments with HFF and BHK-21 cells.

2.3 Culture on microcarriers

Cytodex ™ 1 was used following the manufacturer's recommendations. Cytodex ™ 1 microcarriers (#17044803) were obtained from Cytiva (Uppsala, Sweden). The hydration and sterilisation process of Cytodex ™ 1 were carried out according to the manufacturer's guide "Microcarrier Cell Culture Principles and Methods." Dry Cytodex ™ 1 microcarriers were added to PBS (50 mL/g Cytodex ™ 1) for at least 4 h for hydration, then washed once using the same volume of PBS, and then autoclaved at 121 °C for 30 min. Before use, the sterilised microcarriers were allowed to settle, the supernatant was decanted, and the microcarriers were rinsed in warm culture medium (20–50 mL/g Cytodex ™ 1). Microcarriers (0.20 g of Cytodex ™ 1) were added to 30 mL culture medium, and then CHO-K1 cells recovered from F75 flasks were added at a cell/bead ratio of 50/1. The culture was performed using an Erlenmeyer flask (Corning, Corning, USA) under manual agitation every 30 minutes three times (for 1 h 30), then in continuous agitation at 80 rpm. The final volume was adjusted to 65 mL. After 3 days of culture, tachyzoites were added at MOI 1, and agitation was stopped for 1 h. Protozoa were recovered in the culture supernatant, and beads were removed by filtration using a 40 μm cell strainer (Falcon, Corning, USA).

All the culture steps were performed in DMEM high glucose, 1 % GlutaMAX ™, 10 mM HEPES, 1 % FBS.

2.4 Optical and scanning electron microscopy (SEM) of microcarriers

CHO-K1 growth on microcarriers was estimated using optical and electronic microscopies. For optical microscopy, 0.5 mL was aseptically removed and 1 drop of Nucblue ™ Live stain cell ReadyProbes ™ reagent (Invitrogen, Bothell, USA) was added for 15 min before image acquisition with EVOS M7000 using the lightcube DAPI. For cell counting, 3D images were acquired using the Z-stack function of the EVOS. Cell count was performed by counting blue-stained nuclei on several microcarriers.

For SEM, 2 millilitres of medium were aseptically removed, and cells and microcarriers were recovered by centrifugation for 10 min at 200 g and suspended in 5 mL PBS for washing. Cells were then fixed in Trump fixative buffer for 2 h at room temperature and kept at 4 °C before analysis. Samples were washed in PBS and post-fixed in 1 % osmium tetroxide, dehydrated in graded ethanol baths and dried before observation under a Zeiss Ultra Plus scanning electron microscope (Oberkochen, Germany).

2.5 ATP content

Intracellular ATP was quantified as previously described (Lin et al. 2011). Freshly released protozoa recovered from HFF culture after total lysis of the cells were divided into 2 samples at a concentration of 5.10^6/mL and incubated in culture medium without serum at 37 °C or 25 °C. An aliquot of 5.10^6 protozoa was removed from each sample at the indicated time point (0, 1, 6, and 18 h). Five million protozoa were suspended in 100 µL PBS, and immediately frozen in liquid nitrogen and kept at – 80 °C until ATP quantification. ATP levels from each sample were measured as duplicates in a flat-bottomed white 96-well plate. Fifty microliters of the protozoan suspension, containing 1×10^6 protozoa, was mixed thoroughly with the same volume of BacTiter-Glo ™ reagent (Promega, Madison, USA) and incubated at room temperature for 5 min. Luminescence was detected using luminometry with the GloMax® Navigator Microplate Luminometer (Promega, Madison, USA). Protozoa ATP content was measured and normalised with the ATP content of the sample collected at time 0.

2.6 Determination of invasion efficiency of the protozoa by plaque assay

Invasion was estimated by plaque assay. Briefly, 100 freshly egressed protozoa were inoculated onto a confluent monolayer of HFFs in a 12-well plate and left undisturbed for 8 days at 37 °C and 5 % CO_2.

The supernatants were discarded, and 300 µL of crystal violet solution (0.2 % in 2 % ethanol) (Sigma-Aldrich, Saint Louis, USA) were added and incubated for 20 min at room temperature. Wells were then washed 3 times with tap water and air-dried. Images were acquired using an EVOS ™ M7000 Imaging System (Invitrogen, Bothell, USA). Plaques resulting from cell lysis were manually counted on the entire well.

2.7 CHO-K1 Cells Preparation for kinetic studies

CHO-K1 cells were adapted to culture in Advanced DMEM/F-12. Cells were cultured for three passages post-thawing to ensure recovery and stable growth before experimental use.

Subculturing was performed using accutase® (Sigma-Aldrich, Saint Louis, USA) at room temperature until the cells were completely detached. The cell suspension was collected with fresh medium and centrifuged at 300 × g for 5 min. The supernatant was discarded, and the pellet was resuspended in fresh culture medium and seeded into new flasks.

Cells were subsequently expanded under four different culture conditions: serum-free DMEM/F-12, and supplemented with 0.1 % FBS, 1 % Insulin-Transferrin-Selenium (ITS) and Advanced DMEM/F-12.

Before starting the infection kinetics, cells were distributed at 2.10^5 cells per well in 12-well plates containing 2 mL of culture medium per well.

2.8 Infection of CHO-K1 with *Neospora caninum*

Extracellular tachyzoites recovered from HFF cultures were transferred onto CHO-K1 cell monolayers cultured in Advanced DMEM/F-12 supplemented with 1 % GlutaMAX ™. At the time of infection, CHO-K1 cells displayed approximately 20–30 % confluence. Following infection, the culture medium was replaced with DMEM/F-12 supplemented with 1 % GlutaMAX ™.

At least two consecutive passages of *N. caninum* on CHO-K1 cells were performed before initiating the kinetic experiments to ensure protozoan adaptation to the host cell line. Once harvested, extracellular tachyzoites were counted using a Malassez counting chamber. Before infection, protozoa were resuspended in Dulbecco's Phosphate Buffered Saline (PBS, Clearline, Strasbourg, France) to avoid mixing different culture media. Tachyzoites were then added to CHO-K1 cells previously seeded at 2.10^5 cells/well in 12-well plates after cell adhesion, at various multiplicities of infection (MOI = 1, 2.5, 5, and 10).

2.9 Sample collection for metabolite analyses

At 24, 48, 72, and 96 h of culture, 500 µL of culture medium were aseptically collected from each well and transferred into tubes, which were immediately stored at −20 °C until analysis.

After thawing, culture supernatants were analysed using a Gallery™ automated analyzer (Thermo Fisher Scientific) to quantify glucose and lactate concentrations. Measurements were performed using the Gallery D-Glucose and Gallery L-Lactic Acid kits (Thermofisher) according to the manufacturer’s instructions. Sample dilutions were automatically adjusted by the instrument. Results were expressed as g/L for glucose and mg/L for lactate.

2.10 Calculation of kinetic parameters

Kinetic parameters, including volumetric rates, global rates, and conversion yields, were calculated from the time-course data.

Volumetric rates (*r'''*) were determined by computing the derivative of the analyte concentration with respect to time post-infection. These rates represent the change in concentration per unit of time within the culture medium. To obtain the corresponding global rate (*r*) for each well, the volumetric rate was multiplied by the well volume (2 mL).

Conversion yields (*Y*) were calculated as the ratio of two rates (e.g., product formation rate over substrate consumption rate) to quantify the efficiency of conversion.

For clarity and reproducibility, an example formula is provided for each parameter:

- **Glucose consumption volumetric rate:**

$$r'''_{\text{glucose}} = -\frac{\mathrm{d}[Glucose]}{\mathrm{d}t} = \frac{[Glucose]_{t=0} - [Glucose]}{t}$$

$$r'''_{\text{lactate}} = \frac{\mathrm{d}[Lactate]}{\mathrm{d}t} = \frac{[Lactate] - [Lactate]_{t=0}}{t}$$

- **Global rate:**

$$r_{\text{glucose}} = r'''_{\text{glucose}} \times V_{\text{well}}$$

- **Conversion yield:**

$$Y_{\text{lactate/glucose}} = \frac{r'''_{\text{lactate}}}{r'''_{\text{glucose}}}$$

All calculations were performed for each well and time point to enable the analysis of metabolic kinetics during infection.

2.11 Statistical analyses

Data plotting and statistical analyses were performed using GraphPad Prism software, version 6.0 (GraphPad, San Diego). All statistical tests were two-sided, and a value of $p < 0.05$ was considered statistically significant.

3 Results

3.1 ATP assay as an analytical tool

In a bioproduction process, several analytical tools are required to be set up to monitor the product's integrity throughout the whole production process. As *N. caninum* must remain viable and retain its cell-invasive capacity to exert an anti-tumour effect, invasion potency is the key parameter monitored throughout the production process.

Protozoa need ATP as an energy source, especially to invade cells. *N. caninum* recovered after HFF cell lysis were left undisturbed in medium without serum at 37 °C and 25 °C to fit better with the bioproduction process for different lengths of time (0,1, 6 and 18 h after recovery). Intracellular ATP content was quantified (**Fig. 1**a) at these different times after tachyzoite release from HFF cells. At 37 °C, the ATP content significantly decreased from time 0 at 6 h and 18 h after protozoan release from the cells.

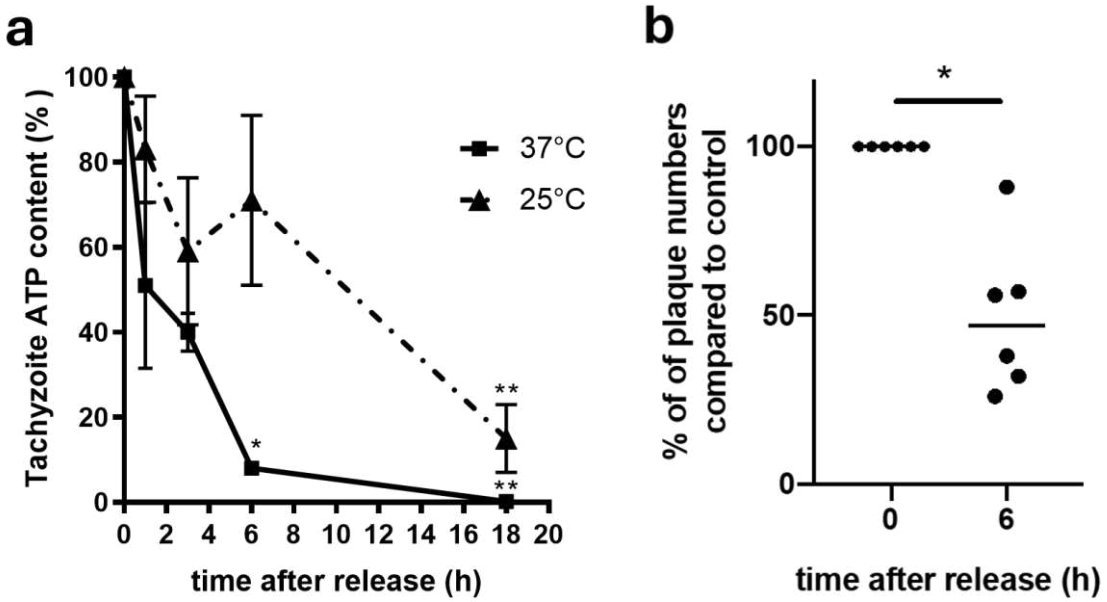


Fig. 1 ATP content of protozoa after release from cell culture and correlation to invasion potency a) Freshly released *N. caninum* were divided into 2 samples and incubated in culture medium at 37 °C (plain line) or 25 °C (dashed line). An aliquot of 5.10^6 parasites was removed from each sample at the indicated time points (0, 1, 6, and 18 h). *N. caninum* ATP content was measured and normalised to the ATP content of the sample collected at time 0. Results are expressed as mean± SEM. (n=2 independent experiments for the 18 h time point to 6 for the 6 h time point). b) Percentage of invasion reduction obtained by plaque assay. Freshly released parasites were

incubated in culture medium at 25 °C, and an aliquot of 100 parasites was removed at time 0 and 6 h after release. Statistical analyses were performed using two-way ANOVA:* < 0.05, **<0.001

At 25 °C, although there was high variability in measurements, the ATP content decreased slightly until 6 h (to less than 60 % from 0) and then dropped significantly to less than 20 % after 18 h in extracellular conditions.

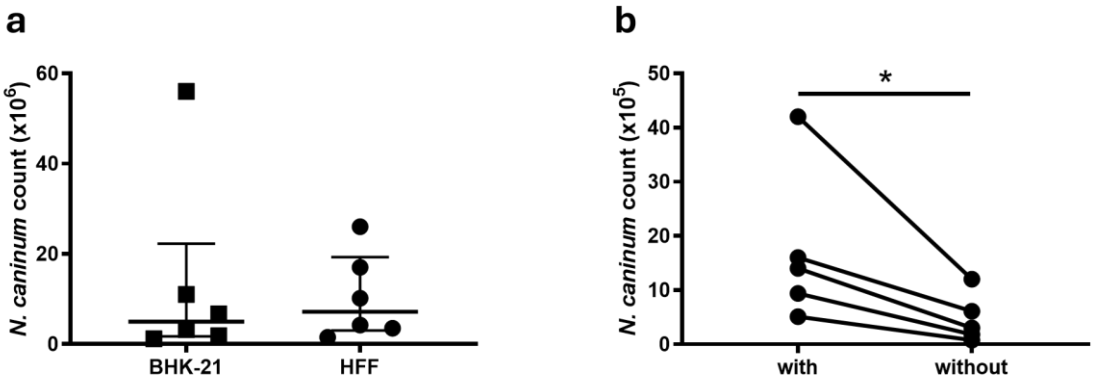
To confirm that ATP is necessary for the invasion step, invasion capacity was assessed by plaque assay to validate protozoan infectivity. Plaque assays were performed at 25 °C, both immediately (0 h) and 6 h after protozoa release from the cells. (**Fig. 1**b). The number of plaques decreased significantly 6 h after egress from 12 to 74 % reduction in comparison to time 0 after protozoa recovery. After 18 h in extracellular conditions, infectivity was completely lost with no plaque detected (data not shown).

These results confirmed that ATP quantification is a good tool to follow the invasion capacity of the protozoa. It also demonstrates that for *N. caninum*, as described for *T. gondii,* the invasion efficiency was almost unaffected by a short incubation period extracellularly (less than 6 hours), suggesting that the whole production process (USP and DSP) should be performed within 6 hours.

3.2 Comparison of protozoa yield on HFF and BHK-21 cell lines

In laboratory conditions, protozoa were cultured on HFF cells, which are fibroblasts derived from human foreskin and are not usually used in bioproduction processes.

BHK-21 cells were chosen for their proximity to HFF and their use in biopharmaceutical processes. Both are fibroblast-like cell types and have a doubling time of around 30 to 50 h. Both cell lines were cultured, after stepwise adaptation, in DMEM medium supplemented with 1% FBS and infected with a multiplicity of infection (MOI) of 2.5. Protozoa were counted in the supernatant of lysed cells 72 h pi. As shown in **Fig. *2***a, there was no significant difference between the 2 cell lines in the number of recovered *N. caninum*.



315

316 **Fig. 2** Comparison of *N. caninum* yield between production on HFF and BHK-21 cells. Cells were
317 seeded at 2.10^5 /well in a 6-well plate in 1 mL DMEM medium. After 4 hours, *N. caninum* were
318 added to the wells at MOI 2.5 in 3 mL final volume. After 72 h of culture protozoa were recovered
319 in the supernatant and counted using a Malassez counting chamber. a) Comparison of yield
320 between HFF and BHK-21 cells (median ± quartile). b) Comparison of culture with or without 1 %
321 FBS during the infection step. Statistical analyses were performed using the Wilcoxon test: *<0.05

322

323 We failed to adapt HFF cells to culture without serum. To observe the effect of serum
324 supplementation on protozoan recovery, the cells were cultured with 1 % FBS and the serum was
325 removed (without) or not (with) for the infection step. Tachyzoite counts were performed 72 h after
326 infection. As shown in **Fig. *2***b, the effect of serum was significant, with reduced yield in the
327 absence of serum during the infection step, regardless of the cell line used (HFF or BHK-21). No
328 significant differences were observed between the two cell lines.

329 To assess the metabolic performance of the cells and the impact of infection, glucose
330 consumption and lactate production were quantified (**Fig. 3**) in the culture supernatants 72 h after
331 the infection. Glucose consumption was significantly different between HFF and BHK-21 for the
332 condition without serum. For HFF cells, no significant consumption was observed (mean 4.4 ±
333 0.1 and 3.91 ± 0.08 g/L without and with serum, respectively) in comparison to the value at t=0
334 (4.5 g/L). For BHK-21 cells, glucose consumption was significantly different from the value at t=0
335 and from that of HFF cells for the conditions without serum (2.24 ± 0.42 g/L). In parallel, lactate
336 production was significantly different from values at t=0 for BHK-21 cells (mean of 30 ± 20 mg/L
337 at t=0, 929 ± 161 mg/L and 583 ± 119 mg/L without and with serum, respectively). Values for both
338 glucose consumption and lactate production with and without protozoa were not significantly
339 different.

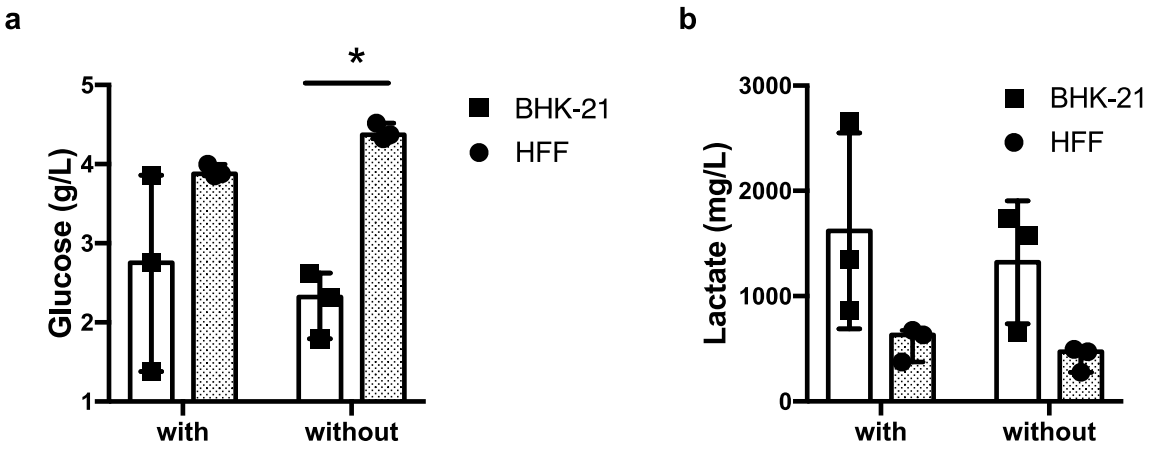
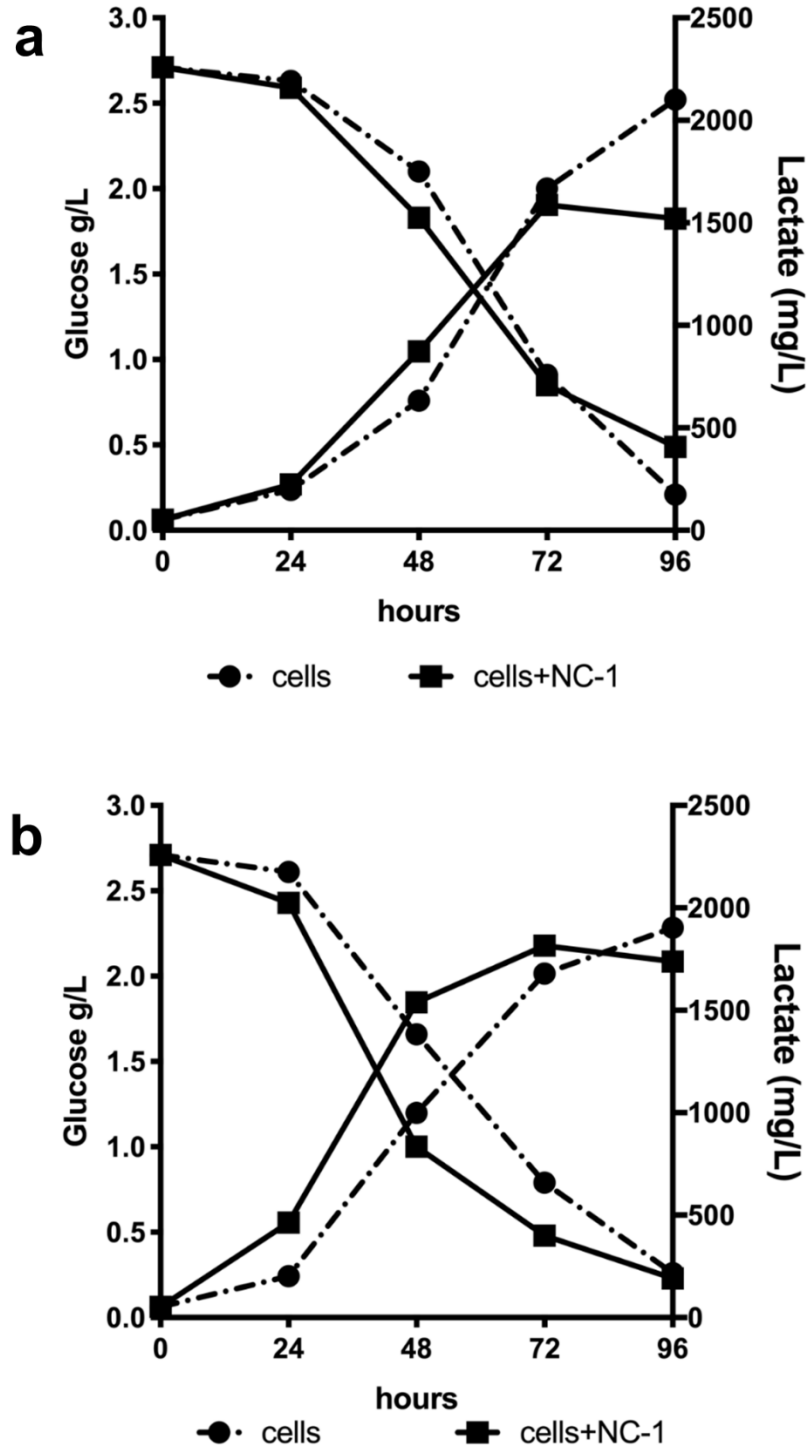


Fig. 3 Comparison of glucose consumption (a) and lactate production (b) in the culture supernatant of HFF and BHK-21 infected cells. Cells were seeded at 2.10^5 /well in 6-well plates in 1 mL DMEM medium. After 4 hours, *N. caninum* were added in the wells at MOI 2.5 in 3 mL final volume without or with serum. At 72 h, supernatant was recovered for glucose and lactate quantification (n=3 independent experiments; values are expressed as mean ± SD).

Glucose consumption and lactate production in these experimental conditions are more related to cell growth rather than to infection since protozoa recoveries were not different between the 2 cell lines. Moreover, BHK-21 cells proliferate rapidly during the 72-h culture time, contrary to HFF cells that stop growing due to contact inhibition.

Altogether, these results suggest that there was no effect of infection at this MOI on glucose consumption and lactate production, regardless of the cell line.

To further confirm these results, kinetics were performed, and glucose consumption (**Fig. 4**a) was first compared between conditions with and without serum until 96 h p.i. in BHK-21 cells infected with *N. caninum*. All cultures were performed in DMEM/F-12, and MOI was 2.5.



355

356 **Fig. 4** Kinetics of glucose consumption and lactate production in culture supernatant of BHK-1
357 cells with and without *N. caninum* infection. Cells were seeded at 2.10^5 /well in 6-wells plate in 1
358 mL DMEM/F12 medium and after 4 hours, *N. caninum* were added in the wells at MOI 2.5 in 3 mL
359 final volume a) without serum and b) with 1 % FBS. Five hundred µL were recovered at different
360 time points from 0 to 96 h of culture for glucose and lactate quantification (one experiment
361 representative of 2 independent experiments)

Glucose consumption increased until being under the threshold of 1 g/L after 72 h of culture in all conditions with and without serum and with and without infection. Lactate production (**Fig. *4***b) also increased with time of culture, reaching between 1500 and 2000 mg/mL at 96 h p.i. in all conditions.

Under these conditions, infection does not seem to change glucose consumption and lactate production since values with and without infection were similar, regardless of the time point.

To further improve the production yield in advanced DMEM/F-12 without serum, several MOIs (from 1 to 50) and several numbers of cells were tested. In all conditions, the protozoan yields were very low (between 1 and 2, **Table S1**)

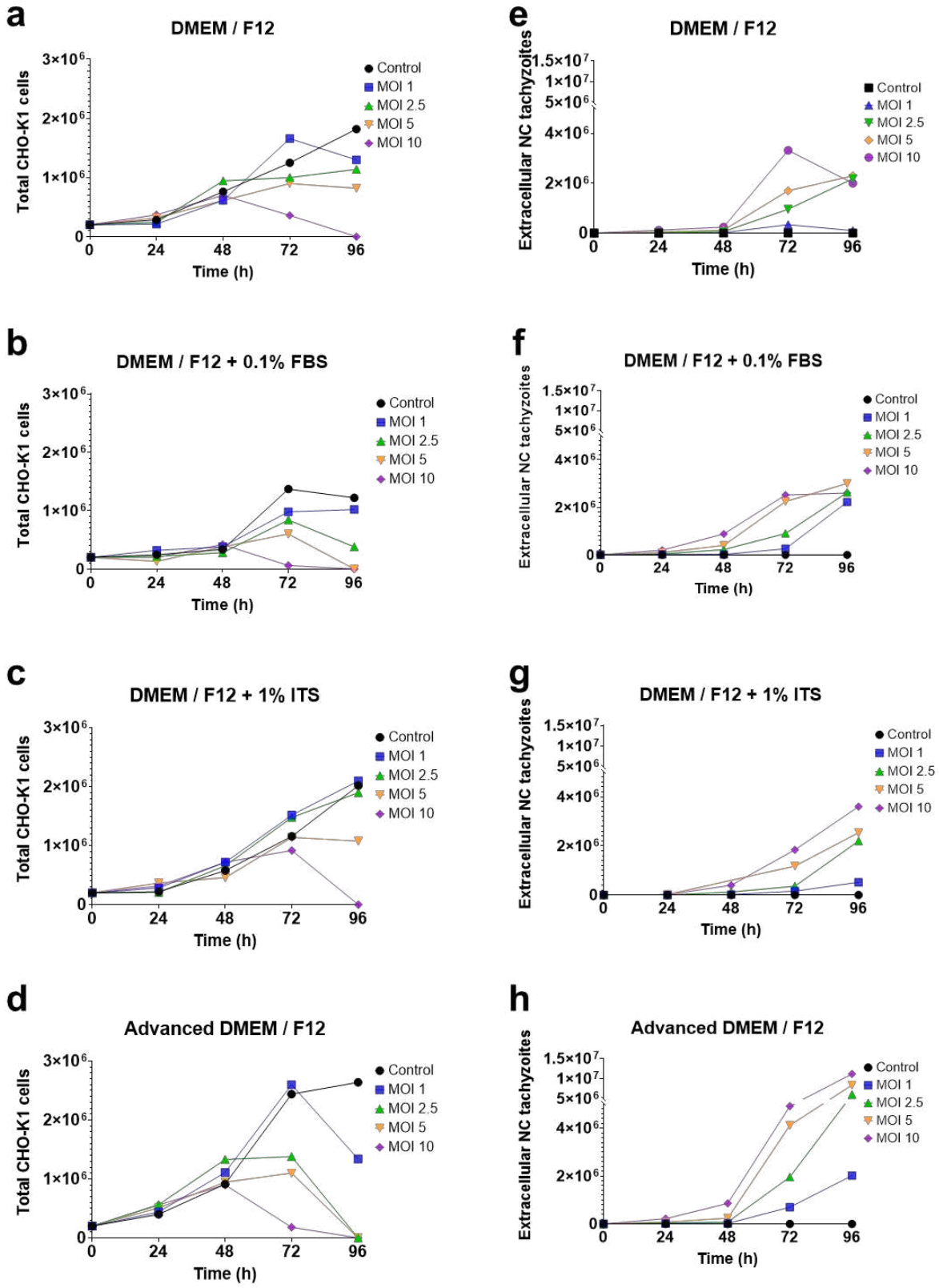
Taking the results together, including the low production yields of the BHK-21 cells and the fact that HFF cells are not suitable for industrial use, a change of host cells was decided. CHO-K1 cells were selected for their widespread use in bioproduction processes and their rapid growth, and all further experiments only used this cell line.

3.3 Influence of *N. caninum* on CHO-K1 growth and substrate metabolism

Due to the limited performance of BHK-21 cells, regardless of MOI, they were replaced by CHO-K1 cells while studying two factors: the culture medium (Advanced DMEM/F12 and DMEM/F12 with its supplemented derivatives) and the MOI.

3.3.1 Influence of culture medium composition and multiplicity of infection on CHO-K1 cell growth and extracellular tachyzoite production

The influence of culture medium composition (Advanced DMEM/F-12, DMEM/F-12, DMEM/F-12 + FBS, DMEM/F-12 + ITS) and MOI on both CHO-K1 cell growth and NC1 extracellular tachyzoite production was monitored over a 96-h cultivation period (**Fig. *5***). Cultures were inoculated with 2 × 10^5 CHO-K1 cells/well, and protozoa released into the culture supernatant were quantified throughout the experiment.



388

389

390 **Fig. 5** Effect of culture medium composition and multiplicity of infection (MOI) on CHO-K1 cell
391 growth and extracellular *N. caninum* tachyzoite production. Total CHO-K1 cell counts per well

were monitored over a 96 h cultivation period in (a) DMEM/F-12, (b) DMEM/F-12 supplemented with 0.1 % FBS, (c) DMEM/F-12 supplemented with 1 % ITS, and (d) Advanced DMEM/F-12. Extracellular tachyzoites released following host cell lysis were quantified in the corresponding culture supernatants for (e) DMEM/F-12, (f) DMEM/F-12 supplemented with 0.1 % FBS, (g) DMEM/F-12 supplemented with 1 % ITS, and (h) Advanced DMEM/F-12. CHO-K1 cells were inoculated at an initial density of 2×10^5 cells per well and infected with *N. caninum* tachyzoites at MOIs of 1, 2.5, 5 or 10. Non-infected cultures were included as controls. n=2

In the absence of infection, CHO-K1 cells proliferated in all four media, although with distinct growth performances. Advanced DMEM/F-12 supported the highest cell expansion, reaching 2.64 $\times 10^6$ cells after 96 h. DMEM/F-12 supplemented with 1 % ITS also promoted robust cell growth (2.02×10^6 cells), whereas basal DMEM/F-12 reached 1.82×10^6 cells. In contrast, DMEM/F-12 supplemented with 0.1 % FBS resulted in the lowest final cell density (1.22×10^6 cells), indicating that this supplementation did not improve host cell expansion under the conditions tested.

Following infection, CHO-K1 cell growth became progressively dependent on the MOI. At MOI 1, host cells continued to proliferate in all media, although final cell numbers were lower than in the corresponding non-infected controls. Increasing the MOI progressively accelerated protozoan-induced cytopathic effects, resulting in an earlier decline in total cell number. At MOIs 5 and 10, complete host cell loss was observed by 96 h in Advanced DMEM/F-12 and DMEM/F-12 supplemented with 0.1 % FBS. In contrast, basal DMEM/F-12 and, more markedly, DMEM/F-12 supplemented with 1 % ITS maintained substantial host cell populations throughout the experiment, with cell numbers of 8.2×10^5 and 10.8×10^5 cells, respectively, at MOI 5.

The kinetics of extracellular tachyzoite accumulation closely reflected the progression of host cell loss. Infected cultures exhibited a progressive increase in tachyzoite number after an initial lag phase. During the first 48 h, the number of extracellular protozoa remained relatively low in all media regardless of the MOI, indicating that most protozoa were still undergoing intracellular replication. A marked increase in extracellular tachyzoite numbers was subsequently observed between 48 and 72 h, coinciding with the onset of reduced host cell numbers in comparison to the non-infected control.

Increasing the MOI accelerated protozoan release throughout the culture period. At 72 h, extracellular tachyzoite concentration already exceeded 3×10^6 protozoa at MOI 10 in basal DMEM/F-12 and reached almost 5×10^6 protozoa in Advanced DMEM/F-12. Differences between culture media became even more pronounced after 96 h. Advanced DMEM/F-12 consistently

yielded the highest extracellular protozoan concentrations, reaching 6.0×10^6, 8.4×10^6 and 11.2×10^6 tachyzoites at MOIs 2.5, 5 and 10, respectively. Basal DMEM/F-12 and DMEM/F-12 supplemented with 0.1 % FBS generated intermediate protozoan numbers, whereas DMEM/F-12 supplemented with 1 % ITS produced comparatively fewer extracellular tachyzoites during the early stages of infection but maintained a more progressive increase throughout the cultivation.

To further compare protozoa propagation, an overall tachyzoite amplification factor was calculated as the ratio between the cumulative number of extracellular tachyzoites recovered during the 96 h cultivation period and the initial protozoa inoculum (**Table *1***). Among the culture media evaluated, Advanced DMEM/F-12 consistently exhibited the highest amplification capacity, yielding multiplication factors of 13.8-, 16.2-, 12.8- and 8.6-fold at MOIs 1, 2.5, 5 and 10, respectively. Notably, the greatest protozoan amplification was achieved at intermediate infection levels, with the highest multiplication factor (16.2-fold) obtained at MOI 2.5, closely followed by MOI 1 (13.8-fold). In comparison, basal DMEM/F-12 and DMEM/F-12 supplemented with 1 % ITS showed lower amplification factors (2.3- and 3.5-fold at MOI 1), whereas DMEM/F-12 supplemented with 0.1 % FBS displayed intermediate performance (12.6-fold at MOI 1). Overall, these results identified Advanced DMEM/F-12 as the most suitable culture medium for *N. caninum* propagation in CHO-K1 cells, providing the highest protozoan amplification while maintaining robust host cell support throughout the production process. Also, it appears that 2.5 is the best MOI under these conditions, regardless of the culture medium.

Table 1 Overall *N. caninum* tachyzoite amplification factor obtained in CHO-K1 cultures under different culture media and multiplicities of infection (MOI). The multiplication factor was calculated as the ratio of the cumulative number of extracellular tachyzoites recovered throughout the cultivation period (96 h) to the initial number of tachyzoites inoculated at t = 0. CHO-K1 cells were cultured in four different media and infected at MOIs of 1, 2.5, 5 or 10. n=1

Medium	MOI 1	MOI 2,5	MOI 5	MOI 10
DMEM / F12	2.3	6.44	4.16	2.84
DMEM / F12 + 0.1 % FBS	12.6	7.56	5.74	3.1
DMEM / F12 + 1 % ITS	3.5	5.36	3.74	2.93
Advanced DMEM / F12	13.8	16.16	12.8	8.6

Overall, the combined analysis of host cell growth and extracellular protozoa accumulation revealed distinct production profiles depending on the culture medium. Advanced DMEM/F-12

clearly maximised both CHO-K1 cell proliferation and protozoa amplification, leading to a rapid host cell loss at high MOIs. Under these conditions, the recovery of all extracellular tachyzoites is achieved rapidly. Conversely, supplementation with 1 % ITS prolonged host cell multiplication, resulting in delayed protozoan release despite sustained protozoan production. These observations highlight the strong interaction between host cell physiology and protozoan replication kinetics during *N. caninum* bioproduction.

3.3.2 Glucose and lactate concentration kinetics

Across all tested culture conditions, the glucose concentration decreased progressively over time in both control and *N. caninum*-infected CHO-K1 cultures (**Fig. 6**). In DMEM/F-12 (**Fig. 6**a) and DMEM/F-12 supplemented with 0.1 % FBS (**Fig. 6**c), glucose consumption was gradual, with slightly lower residual concentrations observed in infected cultures compared to the non-infected controls after 72 hours. In DMEM/F-12 supplemented with ITS (**Fig. 6**e), glucose concentrations showed a more variable trend, with a transient stabilisation or even a slight increase at 48 hours in some infection conditions, followed by a moderate decrease at 72 hours. In contrast, cultures maintained in Advanced DMEM/F-12 (**Fig. 6**g) exhibited a faster and more homogeneous glucose consumption profile for all conditions, reaching minimal residual levels at the end of the kinetics.

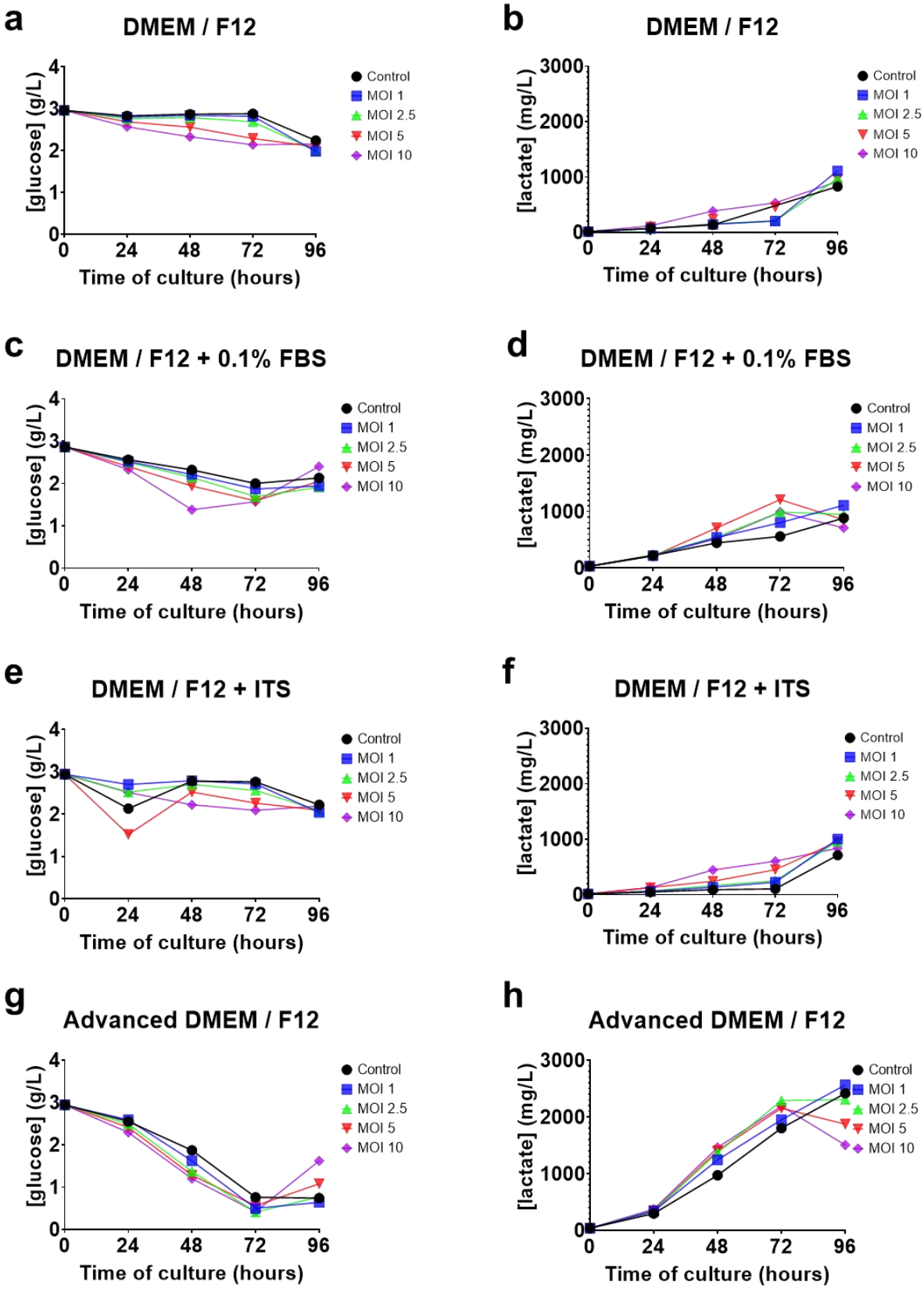


Fig. 6 Time-course profiles of glucose consumption and lactate production in CHO-K1 cell cultures infected with *N. caninum* under different medium conditions. Glucose and lactate

concentrations were measured in culture supernatants at 24 h, 48 h, 72 h, and 96 h. Panels a, c, e, and g show the evolution of glucose concentration over time, while panels b, d, f, and h display the corresponding lactate concentration profiles. Each row corresponds to a specific culture medium: (a-b) DMEM/F-12, (c-d) DMEM/F-12 + 0.1 % FBS, (e-f) DMEM/F-12 + 1 % ITS, and (g-h) Advanced DMEM/F-12. For each condition, the uninfected control is shown in black, and infected CHO-K1 cells are represented according to the multiplicity of infection (MOI): 1 (blue), 2.5 (green), 5 (red), and 10 (purple). n=1

Overall, *N. caninum* infection appeared to accelerate glucose depletion compared to non-infected controls, particularly at higher MOIs (5 and 10). This effect was most pronounced in serum-free or chemically defined media (Advanced DMEM/F-12 and DMEM/F-12 + ITS), suggesting that infection increases metabolic activity or alters host cell and/or tachyzoite glucose use depending on nutrient availability in the medium.

Lactate accumulation followed an opposite trend to glucose depletion, with a progressive increase in concentration throughout the culture period in all conditions. In DMEM/F-12 and DMEM/F-12 + 0.1 % FBS (**Fig. 6**b and d), lactate levels increased, reaching approximately 1000–1500 mg/L after 72 hours in the infected cultures. In the presence of ITS (**Fig. 6**f), lactate production was less pronounced but still elevated in infected conditions compared to the uninfected control. The highest lactate accumulation was observed in Advanced DMEM/F-12 (**Fig. 6**h), where concentrations approached 2000 mg/L at 72 hours, particularly for MOIs 5 and 10.

Taken together, these results indicate that *N. caninum* infection enhances lactate production in CHO-K1 cells in a dose-dependent manner. The extent of this metabolic shift appears to depend on the culture medium composition, being most evident in nutrient-rich, serum-free formulations.

3.3.3 Yield of glucose-to-lactate conversion

Volumetric rates were calculated from linear regressions of glucose and lactate concentrations for each condition, and global rates were derived by scaling to the culture volume (**Fig. S1**, **Table S2**, **Table S3**). Overall, *N. caninum* infection increased both glucose consumption and lactate production rates in an MOI-dependent manner in DMEM/F-12 and in supplemented conditions

(0.1 % FBS or ITS). In contrast, in Advanced DMEM/F-12, both volumetric and global rates remained within a narrower range across MOIs, indicating limited metabolic variation despite infection. The bioconversion yield of glucose to lactate was calculated as the ratio between lactate production and glucose consumption rates (**Table 2**). In most conditions, yields ranged between approximately 500 and 1000 mg lactate per g of glucose consumed, with moderate variations depending on the culture medium and infection level.

Table 2 Yield of glucose-to-lactate conversion in CHO-K1 cultures infected with *N. caninum*. Yields were calculated as the ratio between lactate production and glucose consumption rates, expressed in mg of lactate produced per g of glucose consumed. CHO-K1 cells were cultured in DMEM/F-12, DMEM/F-12 + 0.1 % FBS, DMEM/F-12 + ITS, or Advanced DMEM/F-12 under increasing multiplicities of infection (MOI = 1, 2.5, 5, 10). n=1

Medium	**Yield lactate/glucose (mg of lactate / g of glucose)**				
	Control	**MOI = 1**	**MOI = 2.5**	**MOI = 5**	**MOI = 10**
DMEM / F-12	15.7×10^2	11.0×10^2	6.87×10^2	6.06×10^2	6.09×10^2
DMEM / F-12 + 0.1 % FBS	6.55×10^2	7.62×10^2	7.74×10^2	8.31×10^2	5.49×10^2
DMEM / F-12 + 1 % ITS	5.01×10^2	8.69×10^2	6.14×10^2	6.10×10^2	6.24×10^2
Advanced DMEM / F-12	8.19×10^2	8.20×10^2	8.70×10^2	8.55×10^2	8.25×10^2

In DMEM/F-12, yields decreased with increasing MOI, from 15.7×10^2 mg/g in the control to 6.09×10^2 mg/g at MOI 10, suggesting a shift in carbon flux away from lactate production at higher infection intensities. In contrast, in DMEM/F-12 + 0.1 % FBS and DMEM/F-12 + ITS, yields remained relatively stable across MOIs, fluctuating between 550 and 830 mg/g. In Advanced DMEM/F-12, the conversion yield was remarkably consistent across all infection levels (8.19×10^2–8.70×10^2 mg/g).

Altogether, these results indicate that *N. caninum* infection tends to increase global metabolic rates without proportionally enhancing lactate yield, suggesting that additional metabolic pathways beyond glycolysis might contribute to carbon consumption during infection.

3.3.4 Adaptation to suspension culture

To further increase protozoan recovery and to fulfil conditions required for an industrial process, we set up a culture in suspension. We used microcarriers to intensify *Neospora* production, microcarriers were used to optimise CHO-K1 culture and density by providing uniform nutrient distribution, shear resistance, and protection against necrosis.

Cell growth kinetics on the microcarriers were monitored. CHO-K1 cells were cultured with microcarriers, and the growth was estimated between 0 and 72 h of culture. As illustrated in **Fig. *7***, cells grew until 72 h when the microcarriers were fully covered. The counting of cells using Hoechst staining also showed similar growth kinetics. To further estimate the cell number at the last day of the culture, a sample of microcarriers was recovered at 72 h and cells were obtained after trypsinisation and counted.

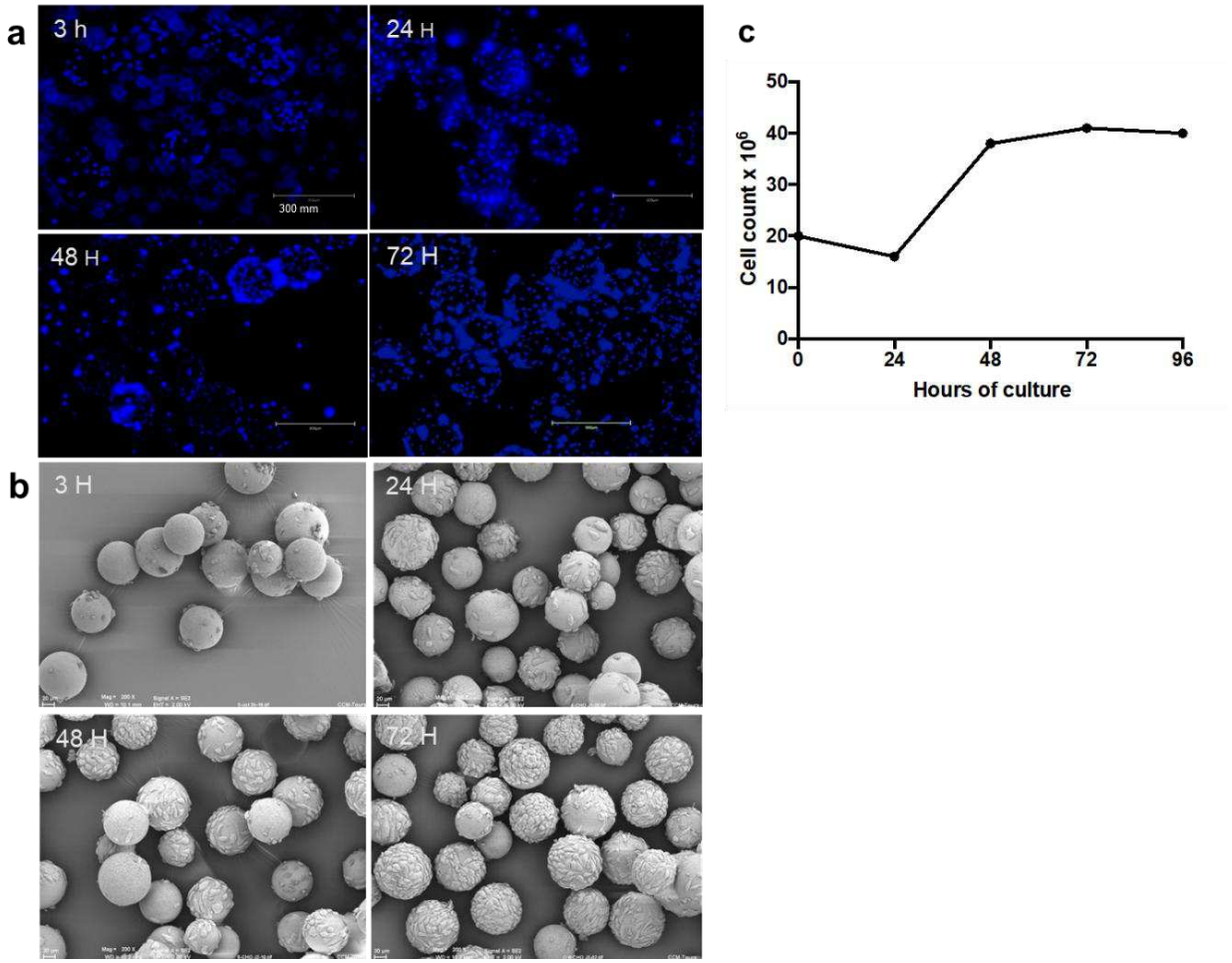


Fig. 7 Production of *T. gondii* on Cytodex ™ 1 microcarriers. (a) Optical microscopy (EVOS M7000, Magnification x20) and (b) SEM of CHO-K1 on Cytodex ™ 1 microcarriers after 3, 24, 48, 72 h of

culture. (c) Cell count after Nucblue reagent staining. Counting was performed on 5 to 30 microcarriers at each time point

N. caninum was added at a ratio of 1:1 and recovered after cell lysis (**Fig. *8***). In this condition, we did not succeed in producing *N. caninum;* in other words, we did not recover any tachyzoites from the culture supernatant. To verify that the microcarrier culture system supports the multiplication of intracellular protozoa, we conducted the experiment under the same conditions using *T. gondii*. Indeed, it has already been produced using HeLa cells on microcarriers (Sağlam Metiner et al. 2019).

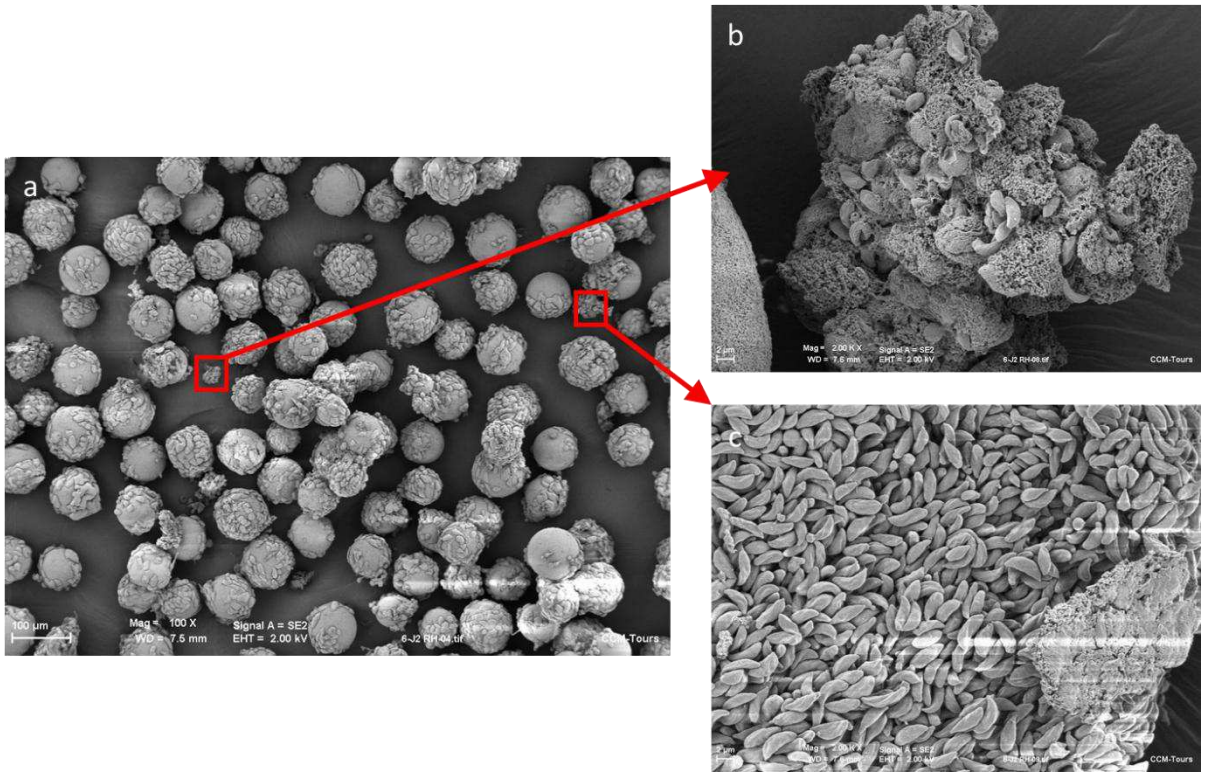


Fig. 8 SEM images of *T. gondii* after 2 days of culture in CHO-K1 adhered to Cytodex ™ 1. (a) Magnification x100. (b) and (c) Magnification x2000. Red boxes and arrows showed tachyzoites

In our conditions, *T. gondii* tachyzoites were recovered in the supernatant 2 to 3 days after addition to the microcarriers. Although these 2 protozoa are closely related, they may have different needs to grow.

Microcarriers represent an innovative technology for large-scale protozoa production; however, optimising their use for *Neospora* remains a challenge.

4 Discussion

The central objective of this work is to explore the feasibility of reducing serum supplementation without negatively impacting the multiplication of the protozoan, which represents a major bottleneck for scalable manufacturing systems.

4.1 Choice of the cell line

N. caninum is able to multiply *in vitro* in a wide range of nucleated mammalian cells, regardless of species or cell type (epithelial, fibroblast, etc). However, production is sensitive to several process parameters, including temperature (Rezende-Gondim et al. 2017), pH and glucose content of the culture medium.

(De Meerschman et al. 2002)We focused on 2 well-characterised adherent cell lines commonly used in bioproduction processes, BHK-21 and CHO-K1, that are adapted to serum-free medium conditions. We successfully produced *N. caninum* in both cell lines in serum-free medium. The same culture medium (advanced DMEM/F-12) was used to support the growth of both cell lines and protozoa. The choice between the 2 cell lines requires consideration of both our experimental results and the available bibliographic data.

BHK-21 cells, which are fibroblasts like the HFFs used in the laboratory for routine NC1 cultures, have been used in the literature to produce *T. gondii* (Grimwood 1980) and CHO-K1 cells to produce NC1 (Nolan et al. 2015). BHK-21 cells have proven to be a suitable production cell line for several viruses and are already used to produce oncolytic viruses (Göbel et al. 2023). We achieved protozoan production using BHK-21 under serum conditions. However, the production yield using this cell line was very low (between 1 and 2-fold). Therefore, a cell line change has been performed in order to increase the amplification factor of the protozoan. CHO-K1 cells have been selected in that case.

CHO cells are among the most widely used cell lines in bioproduction, primarily for recombinant protein production. They are mainly used in the biopharmaceutical industry for the mass production of therapeutic proteins due to advantages such as human-like post-translational modification, correct protein folding, high productivity, and a proven track record in

biopharmaceutical development. Many studies have been conducted to further improve the productivity of these cells, with a recent study developing CHO-MK with a doubling time of 10 h (Masuda et al. 2024). Due to the large amount of data available in the literature on CHO cells and the poor yield obtained with BHK-21 cells, we preferentially performed metabolic analyses and screening of medium and MOI determination on these cells.

4.2 Choice of the culture medium and role of MOI

The present study aimed to evaluate how culture medium composition and infection multiplicity influence the *in vitro* production of *N. caninum* tachyzoites in CHO-K1 cells under reduced-serum or serum-free conditions. NC1 production could be achieved in Advanced DMEM/F-12 (containing albumin) and also with ITS supplement, suggesting that culture could be done without albumin, which could be important for the purification process. Overall, our results demonstrate that protozoan amplification strongly depends on both infection multiplicity and culture medium composition, with Advanced DMEM/F-12 providing the most favourable conditions for tachyzoite production, while supporting robust host cell proliferation before protozoan-induced lysis.

The kinetics of protozoan release observed in this study are consistent with previously reported growth dynamics of *N. caninum in vitro*. In infected cultures, extracellular tachyzoites began to accumulate markedly after approximately 72 h post-infection, coinciding with host cell lysis. Similar growth dynamics have been described in other host cell systems. For example, tachyzoites of the *N. caninum* NC1 isolate cultured in MCF-7 cells showed a rapid increase in extracellular protozoa around day 3 post-infection, reaching maximal levels shortly thereafter, reflecting the completion of intracellular replication cycles followed by host cell rupture (Lv et al. 2010).

Serum is widely used in *N. caninum* culture systems to support host cell growth, but it presents several drawbacks, including batch variability, potential contamination, and the presence of protozoan-reactive antibodies. Indeed, antibodies against *N. caninum* have been detected in commercial foetal bovine serum preparations, demonstrating that serum can introduce biological variability in protozoan culture systems (Torres and Ortega 2006).

Previous work has demonstrated that serum-free chemically defined medium can sustain *N. caninum* tachyzoite production, particularly in Vero cells. De Meerschman et al. (2002) showed that a defined serum-free supplement allowed protozoan propagation with growth patterns comparable to those obtained in serum-containing media, highlighting the feasibility of defined culture systems for protozoan amplification.

More broadly, the development of serum-free systems has been explored for other apicomplexan protozoa. For example, serum-free Vero cell culture has been successfully used to produce large quantities of *T. gondii* tachyzoites while maintaining protozoan infectivity and antigenic properties, demonstrating the potential of defined culture conditions for protozoan production platforms (Da Costa-Silva et al. 2012). But, after a risk assessment, we favour the use of non-primate cell lines in order to mitigate the viral risk.

Within this context, our findings extend previous studies by showing that Advanced DMEM/F-12 can sustain efficient *N. caninum* amplification in CHO-K1 cells with no serum supplementation. This medium supported both robust host cell proliferation during the early phase of infection and high protozoan yields during the lytic phase. The improved performance of this medium likely reflects its optimised formulation, which includes stabilised nutrients and reduced metabolic by-products designed to support high-density mammalian cell cultures.

Interestingly, the superiority of Advanced DMEM/F-12 became particularly evident at higher infection multiplicities, where protozoan yields were markedly higher than in the other tested conditions. This observation suggests that host-cell physiological robustness before lysis is a key determinant of protozoan productivity, as the final number of tachyzoites ultimately depends on the number of infected host cells and their ability to sustain multiple rounds of intracellular replication.

From a bioprocessing perspective, these findings are particularly relevant. The industrial production of intracellular protozoa requires a balance between maximising host cell biomass and optimising protozoan replication kinetics. The infection and multiplication of the protozoan are known to vary depending on the cell line used, with several mammalian cell lines—including Vero and other epithelial cells—showing high permissiveness to *N. caninum* infection (Khordadmehr et al. 2014).

Finally, the ability to produce large quantities of tachyzoites under serum-reduced or serum-free conditions represents an important step toward scalable protozoan production systems. Serum-free media improve reproducibility, reduce regulatory concerns associated with animal-derived components, and facilitate process standardisation in biotechnology applications. Consequently, optimised defined media such as Advanced DMEM/F-12 may provide a promising foundation for the development of controlled and scalable bioproduction platforms for *N. caninum*.

Taken together, our results provide a proof-of-concept that optimised culture media combined with no serum supplementation can significantly improve *N. caninum* tachyzoite production,

opening new perspectives for the development of standardised and scalable protozoan manufacturing processes.

The protozoan amplification factor constitutes an integrative indicator of bioprocess performance, reflecting both host cell permissiveness and protozoan replication over successive lytic cycles. Advanced DMEM/F-12 consistently yielded the highest amplification factors, with optimal performance observed at intermediate MOIs (1 and 2.5), confirming that this medium provides the most favourable environment for *N. caninum* propagation. In contrast, the lower amplification factors obtained at MOI 10 indicate that excessively high protozoan inoculum promotes premature host cell loss, thereby reducing the number of productive replication cycles. These findings demonstrate that maximising the initial protozoan load does not necessarily maximise process performance. From a bioprocess engineering perspective, intermediate MOIs therefore represent the best compromise between inoculum size and protozoan amplification, improving the overall efficiency and potential cost-effectiveness of large-scale *N. caninum* production.

Our results highlight the critical role of infection multiplicity in shaping host cell dynamics and protozoan yield. This is consistent with previous studies demonstrating that intracellular proliferation rates and invasion efficiency are key determinants of protozoan virulence and replication dynamics *in vitro* (Regidor-Cerrillo et al. 2011).

Another integrative indicator of bioprocess performance is the extracellular glucose and lactate dynamics, which have been investigated in this study in CHO-K1 cultures across four media formulations. Three complementary sets of observations emerge from the kinetics, volumetric/global rate calculations and conversion yields: (i) infection generally accelerates glucose depletion and increases lactate accumulation in most media in a dose-dependent fashion; (ii) these metabolic perturbations are medium-dependent, with standard and supplemented DMEM/F-12 showing clear MOI-dependent effects while Advanced DMEM/F-12 shows comparatively attenuated changes between conditions; and (iii) glucose-to-lactate conversion yields do not increase proportionally to the fluxes, suggesting additional fates of carbon or altered metabolic routing under infection.

4.3 Metabolic fluxes as key parameters for bioprocess optimisation

The consistent increase in both glucose consumption and lactate production rates with rising MOI in DMEM/F-12, DMEM/F-12 + 0.1 % FBS, and DMEM/F-12 + ITS suggests a protozoan-associated increase in host glycolytic activity. While these observations are consistent with an

enhanced glycolytic flux, they do not by themselves demonstrate direct metabolic reprogramming of host cells. Nevertheless, this pattern aligns with recent reports indicating that *N. caninum* may modulate host glycolytic pathways, including upregulation of key regulators such as PFKFB3, to support protozoan replication (Tao et al. 2025). More broadly, intracellular apicomplexan protozoa are known to scavenge host nutrients, interfere with metabolic regulation, and impose biosynthetic demands that are often associated with increased reliance on aerobic glycolysis (a "Warburg-like" phenotype), as described for *T. gondii* and related pathogens (Gallego-López et al. 2024). In this context, the elevated glucose uptake and lactate production observed may reflect a combination of host metabolic responses and protozoan-driven demands rather than a strictly defined glycolytic shift (Llibre et al. 2021)

Beyond their biological significance, glucose consumption and lactate production constitute valuable quantitative descriptors for the development and optimisation of a robust *Neospora caninum* bioproduction process. While these metabolites are traditionally monitored to evaluate mammalian cell physiology, they also provide direct information on nutrient demand, metabolic activity and culture performance, all of which are essential parameters in bioprocess engineering (Mulukutla et al. 2016, 2010). In the case of an obligate intracellular protozoan, whose replication entirely depends on host cell metabolism, extracellular metabolite monitoring represents a simple and non-invasive strategy to assess the physiological state of the culture while simultaneously following protozoan propagation.

Our results demonstrate that *N. caninum* infection increased glucose consumption and lactate production in CHO-K1 cultures in an MOI-dependent manner, confirming that protozoan replication imposes an additional metabolic burden on the host cell. Similar metabolic adaptations have been described for several apicomplexan protozoa, which rely heavily on host-derived nutrients and exhibit elevated glycolytic activity during intracellular development (Elsheikha et al. 2020). However, the magnitude of these metabolic changes was strongly influenced by the culture medium, highlighting that protozoan propagation is closely coupled to the nutritional environment provided to the host cells.

The four media evaluated in this study differ in the complexity of their formulations. Whereas basal DMEM/F-12 and its supplemented variants provide relatively conventional nutritional environments, Advanced DMEM/F-12 has been specifically formulated to sustain mammalian cell cultures under reduced-serum conditions. This medium contains chemically defined supplements including insulin, transferrin, selenium and glutathione. These components are known to stimulate glucose uptake, maintain iron homeostasis, reinforce antioxidant defences

and preserve mitochondrial function, thereby improving the metabolic robustness of CHO cells under culture stress (Mulukutla et al. 2016; Coulet et al. 2022). Although the individual contribution of each supplement cannot be distinguished in the present study, their combined action most likely explains the superior host cell expansion, the highest protozoan amplification factors and the comparatively stable extracellular metabolic profiles observed in Advanced DMEM/F-12.

Interestingly, despite supporting the highest protozoan production, Advanced DMEM/F-12 exhibited only limited variations in glucose consumption and lactate production rates across the different MOIs. This apparent metabolic stability suggests that the optimised formulation efficiently accommodates the increasing metabolic demand imposed by protozoan replication while maintaining favourable conditions for both host cell viability and protozoan propagation. In contrast, the larger metabolic variations observed in other media suggest that nutrient availability progressively becomes limiting as infection progresses, resulting in greater perturbations of host cell metabolism.

From a bioprocess engineering perspective, the calculation of glucose consumption rates, lactate production rates and glucose-to-lactate conversion yields provides substantially more information than metabolite concentration profiles alone. These parameters constitute quantitative process descriptors that can readily be incorporated into predictive models describing nutrient utilisation and metabolic activity during protozoan production. Such models could support the rational design of feeding strategies aimed at maintaining glucose concentrations above critical thresholds while limiting excessive lactate accumulation, two variables routinely monitored during industrial mammalian cell culture processes (Teixeira et al. 2009; Mulukutla et al. 2010). Likewise, glucose-to-lactate conversion yields provide valuable information on carbon partitioning and metabolic efficiency, facilitating objective comparisons between culture conditions and revealing metabolic shifts associated with protozoan infection.

Beyond process optimisation, these parameters are particularly attractive within a Quality-by-Design (QbD) framework. Continuous or at-line monitoring of glucose and lactate is already widely implemented in biopharmaceutical manufacturing as part of Process Analytical Technology (PAT) strategies (Sommeregger et al. 2017; Teixeira et al. 2009). Applied to *N. caninum* bioproduction, these measurements could serve as critical process indicators and feed predictive models or soft sensors capable of estimating protozoan propagation, anticipating nutrient depletion and identifying the optimal harvest time without relying exclusively on

microscopic protozoan enumeration (Luttmann et al. 2012). Such approaches would considerably improve process robustness while facilitating future scale-up and automation.

To our knowledge, this is the first study proposing extracellular metabolic fluxes as quantitative process descriptors for the bioproduction of an obligate intracellular protozoan. Although further investigations combining extracellular metabolite analysis with intracellular metabolomics or stable isotope tracing would provide a more comprehensive understanding of host–protozoan carbon partitioning, the methodology presented here already offers practical tools for process development. More broadly, integrating metabolic monitoring, kinetic modelling and predictive control represents a promising strategy for establishing rational, scalable and economically sustainable production processes not only for *N. caninum*, but also for other obligate intracellular protozoa intended for biomedical applications.

Several limitations should nevertheless be considered. First, extracellular glucose and lactate measurements represent global metabolic readouts integrating both host cell and protozoan metabolism, without distinguishing their respective contributions or accounting for potential lactate reutilization. Second, flux calculations rely on linear regressions and may therefore overlook transient metabolic shifts occurring during the cultivation period. Finally, changes in host cell number and viability during infection may affect flux normalisation, while the reduced impact of MOI observed in Advanced DMEM/F-12 could reflect either improved metabolic buffering or differences in protozoan replication. Combining extracellular metabolite analysis with protozoan burden quantification and intracellular metabolomics would help disentangle these effects and provide a more comprehensive understanding of host–protozoan metabolic interactions.

4.4 Technology transfer from adherent to suspension culture

From an industrial point of view, the use of suspension cells may be preferred. Manufacturing can be shifted toward suspension cells using chemically defined media. Suspension cells allow for easy scale-up and passaging while maintaining rapid cell growth.

Both BHK-21 and CHO-K1 cell lines are adapted to suspension growth in serum-free medium. However, infection of the host cell by *N. caninum* tachyzoites is a process which is preceded by adhesion to the host cell surface. The comparison between adherent-growing BHK-21 cells and suspension cells revealed differences in the expression of cellular receptors such as integrins and heparan sulphates (Dill et al. 2021). *N. caninum* tachyzoites bind to sulphated proteoglycans,

including heparin/heparan sulphate, chondroitin sulphates and also exploit sialic acids for attachment and host cell entry. Consequently, adhesion and invasion of NC1 to these suspension-adapted cells may be affected. To bypass this, adherent cells may be cultured on carriers in fixed-bed bioreactors.

The use of microcarriers enables anchorage-dependent animal cells to grow in suspension cultures, in either a batch or perfusion culture format. It enables an increase in the surface area of monolayer cultures. *T. gondii* culture has already been performed using Cytodex ™ 1 and HeLa producer cells (Sağlam Metiner et al. 2019). Based on this publication, we succeeded in producing *T. gondii* using Cytodex ™ 1 on CHO-K1 cells with reduced serum percentage (1 %). However, using the same conditions, we were unable to obtain *N. caninum* tachyzoites. Several hypotheses may explain this difference. Although gene content and expression are conserved between the two protozoa, differences in host preference exist (Al-Bajalan et al. 2017; Cowper et al. 2012). *N. caninum* has a more limited host range than *T. gondii,* and comparisons of genomes and transcriptomes suggest that, for example, the larger number of surface proteins involved in cell attachment may account for the narrower host range of *N. caninum*. This may also restrain attachment to cells *in vitro*. Nolan et al. (2015) have also observed that although *T. gondii* (RH strain) and *N. caninum* (Liverpool strain; Nc-Liv) had similar strategies to exploit cell resources, Nc-Liv grows more slowly in culture regardless of cell origin.

In this study, we have determined that several parameters are essential for process optimisation, such as the choice of the medium, the cell line and the MOI. Despite this, further optimisation paths remain possible.

Exploring cellular metabolism could be a powerful approach to gain insight into the relationship between nutrient consumption and cell growth/protozoa production and further optimise the formulation of culture media. Also, the knowledge of nutrient needs for the host-protozoa system could be useful for process optimisation via a design of experiments approach (DoE) and for the development of a process analytical technology strategy.

Taken together, this work provides a concrete proof-of-concept for the development of an industrially relevant bioprocess for *Neospora caninum* production. The combination of CHO-K1 cells, serum-free or chemically defined media, and controlled infection strategies (notably intermediate MOIs) establishes a robust and scalable framework aligned with current biopharmaceutical manufacturing standards. Beyond demonstrating feasibility, the identification of metabolic fluxes as actionable process parameters opens the way to the implementation of monitoring and control strategies compatible with Quality-by-Design and

Process Analytical Technology approaches. Although further developments will be required to enable full scale-up—particularly regarding suspension culture, cell–protozoan interaction constraints, and bioreactor integration—this study lays the foundation for a standardised, reproducible, and economically viable production platform for *N. caninum*, bridging the gap between laboratory-scale culture and industrial biomanufacturing.

Author Contributions

AM designed the research. CP, NM and ZL conceived and designed the research and conducted experiments. IDP designed the research and participated in the writing. ADT and CD participated in the writing. CP and NM analysed data and wrote the manuscript. All authors read and approved the manuscript.

Funding

This work was funded by the University of Tours and INRAE as part of recurring grants.

Acknowledgments

We thank Armand Bez (IRFTLM, Tours) for his valuable technical contribution during his internship, particularly for his involvement in the experiments performed on BHK-21 cells.

We thank Francis Poisson and the Bio^3 Institute for allowing us to use some of the equipment in the technical facility.

The electron microscopy data were obtained with the assistance of the IBiSA Electron Microscopy Facility of the University of Tours. We thank Sonia Georgeault for her valuable contribution to this microscopy work.

English editing has been performed using Grammarly for macOS software.

Conflicts of interest

All authors declare that they have no conflicts of interest.

References

Al-Bajalan, Mariwan M. M., Dong Xia, Stuart Armstrong, Nadine Randle, and Jonathan M. Wastling. 2017. "*Toxoplasma Gondii* and *Neospora Caninum* Induce Different Host Cell Responses at Proteome-Wide Phosphorylation Events; a Step Forward for Uncovering the

Biological Differences between These Closely Related Parasites." *Parasitology Research* 116 (10): 2707–19. https://doi.org/10.1007/s00436-017-5579-7.

Battistoni, Arthur, Louis Lantier, Anne Di Tommaso, et al. 2023. "Nasal Administration of Recombinant *Neospora Caninum* Secreting IL-15/IL-15Rα Inhibits Metastatic Melanoma Development in Lung." *Journal for ImmunoTherapy of Cancer* 11 (5): e006683. https://doi.org/10.1136/jitc-2023-006683.

Chiappino-Pepe, Anush, Stepan Tymoshenko, Meriç Ataman, Dominique Soldati-Favre, and Vassily Hatzimanikatis. 2017. "Bioenergetics-Based Modeling of *Plasmodium Falciparum* Metabolism Reveals Its Essential Genes, Nutritional Requirements, and Thermodynamic Bottlenecks." *PLOS Computational Biology* 13 (3): e1005397. https://doi.org/10.1371/journal.pcbi.1005397.

Coulet, Mathilde, Oliver Kepp, Guido Kroemer, and Stéphane Basmaciogullari. 2022. "Metabolic Profiling of CHO Cells during the Production of Biotherapeutics." *Cells* 11 (12): 1929. https://doi.org/10.3390/cells11121929.

Cowper, Ben, Stephen Matthews, and Fiona Tomley. 2012. "The Molecular Basis for the Distinct Host and Tissue Tropisms of Coccidian Parasites." *Molecular and Biochemical Parasitology* 186 (1): 1–10. https://doi.org/10.1016/j.molbiopara.2012.08.007.

Da Costa-Silva, Thaís Alves, Cristina Da Silva Meira, Neuza Frazzatti-Gallina, and Vera Lucia Pereira-Chioccola. 2012. "*Toxoplasma Gondii* Antigens: Recovery Analysis of Tachyzoites Cultivated in Vero Cell Maintained in Serum Free Medium." *Experimental Parasitology* 130 (4): 463–69. https://doi.org/10.1016/j.exppara.2012.01.005.

Dalton, John P., Corine G. Demanga, Sarah J. Reiling, Juliane Wunderlich, Jenny W. L. Eng, and Petra Rohrbach. 2012. "Large-Scale Growth of the *Plasmodium Falciparum* Malaria Parasite in a Wave Bioreactor." *International Journal for Parasitology* 42 (3): 215–20. https://doi.org/10.1016/j.ijpara.2012.01.001.

De Meerschman, François, Chantal Rettigner, Charles Focant, et al. 2002. "Use of a Serum-Free Medium to Produce in Vitro *Neospora Caninum* and *Toxoplasma Gondii* Tachyzoites on Vero Cells." *Veterinary Research* 33 (2): 159–68. https://doi.org/10.1051/vetres:2002004.

Débare, Héloïse, Nathalie Moiré, Céline Ducournau, et al. 2021. "*Neospora Caninum* Glycosylphosphatidylinositols Used as Adjuvants Modulate Cellular Immune Responses Induced in Vitro by a Nanoparticle-Based Vaccine." *Cytokine* 144 (August): 155575. https://doi.org/10.1016/j.cyto.2021.155575.

Dill, Veronika, Florian Pfaff, Aline Zimmer, Martin Beer, and Michael Eschbaumer. 2021. "Adherent and Suspension Baby Hamster Kidney Cells Have a Different Cytoskeleton and Surface Receptor Repertoire." *PLOS ONE* 16 (6): e0246610. https://doi.org/10.1371/journal.pone.0246610.

Dubey, J. P., G. Schares, and L. M. Ortega-Mora. 2007. "Epidemiology and Control of Neosporosis and *Neospora Caninum*." *Clinical Microbiology Reviews* 20 (2): 323–67. https://doi.org/10.1128/CMR.00031-06.

Elsheikha, Hany M., Mamdowh Alkurashi, Suzy Palfreman, et al. 2020. "Impact of *Neospora Caninum* Infection on the Bioenergetics and Transcriptome of Cerebrovascular Endothelial Cells." *Pathogens* 9 (9): 710. https://doi.org/10.3390/pathogens9090710.

892 European Medicines Agency. 2013. *Guideline on the Use of Bovine Serum in the Manufacture of*
893 *Human Biological Medicinal Products*. no. EMA/CHMP/BWP/457920/2012 Rev 1.
894 https://www.ema.europa.eu/en/documents/scientific-guideline/guideline-use-bovine-
895 serum-manufacture-human-biological-medicinal-products-revision-1_en.pdf.

896 Gallego-López, Gina M., Emmanuel Contreras Guzman, Danielle E. Desa, Laura J. Knoll, and
897 Melissa C. Skala. 2024. "Metabolic Changes in *Toxoplasma Gondii* -Infected Host Cells
898 Measured by Autofluorescence Imaging." *mBio* 15 (8): e00727-24.
899 https://doi.org/10.1128/mbio.00727-24.

900 Göbel, Sven, Karim E. Jaén, Marie Dorn, et al. 2023. "Process Intensification Strategies toward
901 Cell Culture-based High-yield Production of a Fusogenic Oncolytic Virus." *Biotechnology*
902 *and Bioengineering* 120 (9): 2639–57. https://doi.org/10.1002/bit.28353.

903 Grimwood, B. G. 1980. "Infective *Toxoplasma Gondii* Trophozoites Attenuated by Ultraviolet
904 Irradiation." *Infection and Immunity* 28 (2): 532–35. https://doi.org/10.1128/iai.28.2.532-
905 535.1980.

906 Guerriaud, Mathieu, Cyril Poupet, Zineb Lakhrif, Evelyne Kohli, and Nathalie Moiré. 2024. "Are
907 Genetically Modified Protozoa Eligible for ATMP Status? Concerning the Legal
908 Categorization of an Oncolytic Protozoan Drug Candidate." *Gene Therapy*, ahead of print.
909 https://doi.org/10.1038/s41434-024-00445-1.

910 Khordadmehr, M., M. Namavari, and A. Khodakaram-Tafti. 2014. "Susceptibility of Various Cell
911 Lines to *Neospora Caninum* Tachyzoites Cultivation." *Archives of Razi Institute*.
912 https://doi.org/10.7508/ari.2014.01.008.

913 Krishnan, Aarti, Joachim Kloehn, Matteo Lunghi, et al. 2020. "Functional and Computational
914 Genomics Reveal Unprecedented Flexibility in Stage-Specific *Toxoplasma* Metabolism."
915 *Cell Host & Microbe* 27 (2): 290-306.e11. https://doi.org/10.1016/j.chom.2020.01.002.

916 Lantier, Louis, Agathe Poupée-Beaugé, Anne di Tommaso, et al. 2020. "*Neospora Caninum:* A
917 New Class of Biopharmaceuticals in the Therapeutic Arsenal against Cancer." *Journal for*
918 *ImmunoTherapy of Cancer* 8 (2): e001242. https://doi.org/10.1136/jitc-2020-001242.

919 Li, Xiaojin, Meng Qi, Kai He, et al. 2022. "*Neospora Caninum* Inhibits Tumor Development by
920 Activating the Immune Response and Destroying Tumor Cells in a B16F10 Melanoma
921 Model." *Parasites & Vectors* 15 (1): 332. https://doi.org/10.1186/s13071-022-05456-8.

922 Lin, San San, Martin Blume, Nicolas Von Ahsen, Uwe Gross, and Wolfgang Bohne. 2011.
923 "Extracellular *Toxoplasma Gondii* Tachyzoites Do Not Require Carbon Source Uptake for
924 ATP Maintenance, Gliding Motility and Invasion in the First Hour of Their Extracellular
925 Life." *International Journal for Parasitology* 41 (8): 835–41.
926 https://doi.org/10.1016/j.ijpara.2011.03.005.

927 Llibre, Alba, Frances S. Grudzinska, Matthew K. O'Shea, et al. 2021. "Lactate Cross-Talk in Host–
928 Pathogen Interactions." *Biochemical Journal* 478 (17): 3157–78.
929 https://doi.org/10.1042/BCJ20210263.

930 Luttmann, Reiner, Daniel G. Bracewell, Gesine Cornelissen, et al. 2012. "Soft Sensors in
931 Bioprocessing: A Status Report and Recommendations." *Biotechnology Journal* 7 (8):
932 1040–48. https://doi.org/10.1002/biot.201100506.

Lv, Qiang, Jianhua Li, Pengtao Gong, Shenyang Xing, and Xichen Zhang. 2010. "*Neospora Caninum*: In Vitro Culture of Tachyzoites in MCF-7 Human Breast Carcinoma Cells." *Experimental Parasitology* 126 (4): 536–39. https://doi.org/10.1016/j.exppara.2010.06.006.

Masuda, Kenji, Michi Kubota, Yuto Nakazawa, et al. 2024. "Establishment of a Novel Cell Line, CHO-MK, Derived from Chinese Hamster Ovary Tissues for Biologics Manufacturing." *Journal of Bioscience and Bioengineering* 137 (6): 471–79. https://doi.org/10.1016/j.jbiosc.2024.02.005.

Moleirinho, Mafalda G., Ricardo J. S. Silva, Paula M. Alves, Manuel J. T. Carrondo, and Cristina Peixoto. 2019. "Current Challenges in Biotherapeutic Particles Manufacturing." *Expert Opinion on Biological Therapy* 20 (5): 451–65. https://doi.org/10.1080/14712598.2020.1693541.

Mulukutla, Bhanu Chandra, Salmaan Khan, Alex Lange, and Wei-Shou Hu. 2010. "Glucose Metabolism in Mammalian Cell Culture: New Insights for Tweaking Vintage Pathways." *Trends in Biotechnology* 28 (9): 476–84. https://doi.org/10.1016/j.tibtech.2010.06.005.

Mulukutla, Bhanu Chandra, Andrew Yongky, Tung Le, Douglas G. Mashek, and Wei-Shou Hu. 2016. "Regulation of Glucose Metabolism – A Perspective From Cell Bioprocessing." *Trends in Biotechnology* 34 (8): 638–51. https://doi.org/10.1016/j.tibtech.2016.04.012.

Nolan, Sabrina J., Julia D. Romano, Thomas Luechtefeld, and Isabelle Coppens. 2015. "*Neospora Caninum* Recruits Host Cell Structures to Its Parasitophorous Vacuole and Salvages Lipids from Organelles." *Eukaryotic Cell* 14 (5): 454–73. https://doi.org/10.1128/EC.00262-14.

Pawliw, Rebecca, Rebecca Farrow, Silvana Sekuloski, et al. 2018. "A Bioreactor System for the Manufacture of a Genetically Modified *Plasmodium Falciparum* Blood Stage Malaria Cell Bank for Use in a Clinical Trial." *Malaria Journal* 17 (1): 283. https://doi.org/10.1186/s12936-018-2435-x.

Pol, Jonathan, Guido Kroemer, and Lorenzo Galluzzi. 2016. "First Oncolytic Virus Approved for Melanoma Immunotherapy." *OncoImmunology* 5 (1): e1115641. https://doi.org/10.1080/2162402X.2015.1115641.

Regidor-Cerrillo, Javier, Mercedes Gómez-Bautista, Itsaso Sodupe, et al. 2011. "In Vitro Invasion Efficiency and Intracellular Proliferation Rate Comprise Virulence-Related Phenotypic Traits of *Neospora Caninum*." *Veterinary Research* 42 (1): 41. https://doi.org/10.1186/1297-9716-42-41.

Reid, Adam James, Sarah J. Vermont, James A. Cotton, et al. 2012. "Comparative Genomics of the Apicomplexan Parasites *Toxoplasma Gondii* and *Neospora Caninum*: Coccidia Differing in Host Range and Transmission Strategy." *PLoS Pathogens* 8 (3): e1002567. https://doi.org/10.1371/journal.ppat.1002567.

Rezende-Gondim, Mariana M., Aristeu V. Da Silva, Gereon Schares, and Luís F. P. Gondim. 2017. "In Contrast to *Toxoplasma Gondii*, *Neospora Caninum* Tachyzoites Did Not Sustain Multiplication in Vitro at Increased Incubation Temperatures." *Veterinary Parasitology* 234 (January): 19–24. https://doi.org/10.1016/j.vetpar.2016.12.013.

Sağlam Metiner, Pelin, Hüseyin Can, Duygu Ayyıldız Tamiş, et al. 2019. “The Use of *Toxoplasma Gondii* Tachyzoites Produced in HeLa Cells Adhered to Cytodex 1 Microcarriers as Antigen in Serological Assays: An Application of Microcarrier Technology.” *Cytotechnology* 71 (1): 91–105. https://doi.org/10.1007/s10616-018-0269-6.

Sfakianos, John P., Berengere Salome, Jorge Daza, Adam Farkas, Nina Bhardwaj, and Amir Horowitz. 2021. “Bacillus Calmette-Guerin (BCG): Its Fight against Pathogens and Cancer.” *Urologic Oncology: Seminars and Original Investigations* 39 (2): 121–29. https://doi.org/10.1016/j.urolonc.2020.09.031.

Sommeregger, Wolfgang, Bernhard Sissolak, Kulwant Kandra, Moritz Von Stosch, Martin Mayer, and Gerald Striedner. 2017. “Quality by Control: Towards Model Predictive Control of Mammalian Cell Culture Bioprocesses.” *Biotechnology Journal* 12 (7): 1600546. https://doi.org/10.1002/biot.201600546.

Tao, De-Liang, Jin-Ming Chen, Jiang-Ping Wu, et al. 2025. “*Neospora Caninum* Hijacks Host PFKFB3-Driven Glycolysis to Facilitate Intracellular Propagation of Parasites.” *Veterinary Research* 56 (1). https://doi.org/10.1186/s13567-025-01524-w.

Teixeira, A. P., R. Oliveira, P. M. Alves, and M. J. T. Carrondo. 2009. “Advances in On-Line Monitoring and Control of Mammalian Cell Cultures: Supporting the PAT Initiative.” *Biotechnology Advances* 27 (6): 726–32. https://doi.org/10.1016/j.biotechadv.2009.05.003.

Torres, Maria P., and Ynes R. Ortega. 2006. “*Neospora Caninum* Antibodies in Commercial Fetal Bovine Serum.” *Veterinary Parasitology* 140 (3–4): 352–55. https://doi.org/10.1016/j.vetpar.2006.03.032.

Tymoshenko, Stepan, Rebecca D. Oppenheim, Rasmus Agren, Jens Nielsen, Dominique Soldati-Favre, and Vassily Hatzimanikatis. 2015. “Metabolic Needs and Capabilities of *Toxoplasma Gondii* through Combined Computational and Experimental Analysis.” *PLOS Computational Biology* 11 (5): e1004261. https://doi.org/10.1371/journal.pcbi.1004261.

Vuscan, Patricia, Brenda Kischkel, Leo A. B. Joosten, and Mihai G. Netea. 2025. “Microbial-Induced Trained Immunity for Cancer Immunotherapy.” *Pharmacological Reviews* 77 (5): 100074. https://doi.org/10.1016/j.pharmr.2025.100074.

SUPPLEMENTARY DATA

Table S1 Overall *N. caninum* tachyzoite multiplication factor obtained in BHK-21 cultures in serum-free advanced DMEM/F12 medium under different multiplicities of infection (MOI). The multiplication factor was calculated as the ratio of the cumulative number of extracellular tachyzoites recovered throughout the cultivation period (96 h) to the initial number of tachyzoites inoculated at t = 0. n is the number of independent experiments.

MOI	Multiplication factor
2.5	0.5 (n=1)
5	1.3±0.2 (n=2)
10	2.0±1.6(n=3)
20	1.4±0.4(n=2)

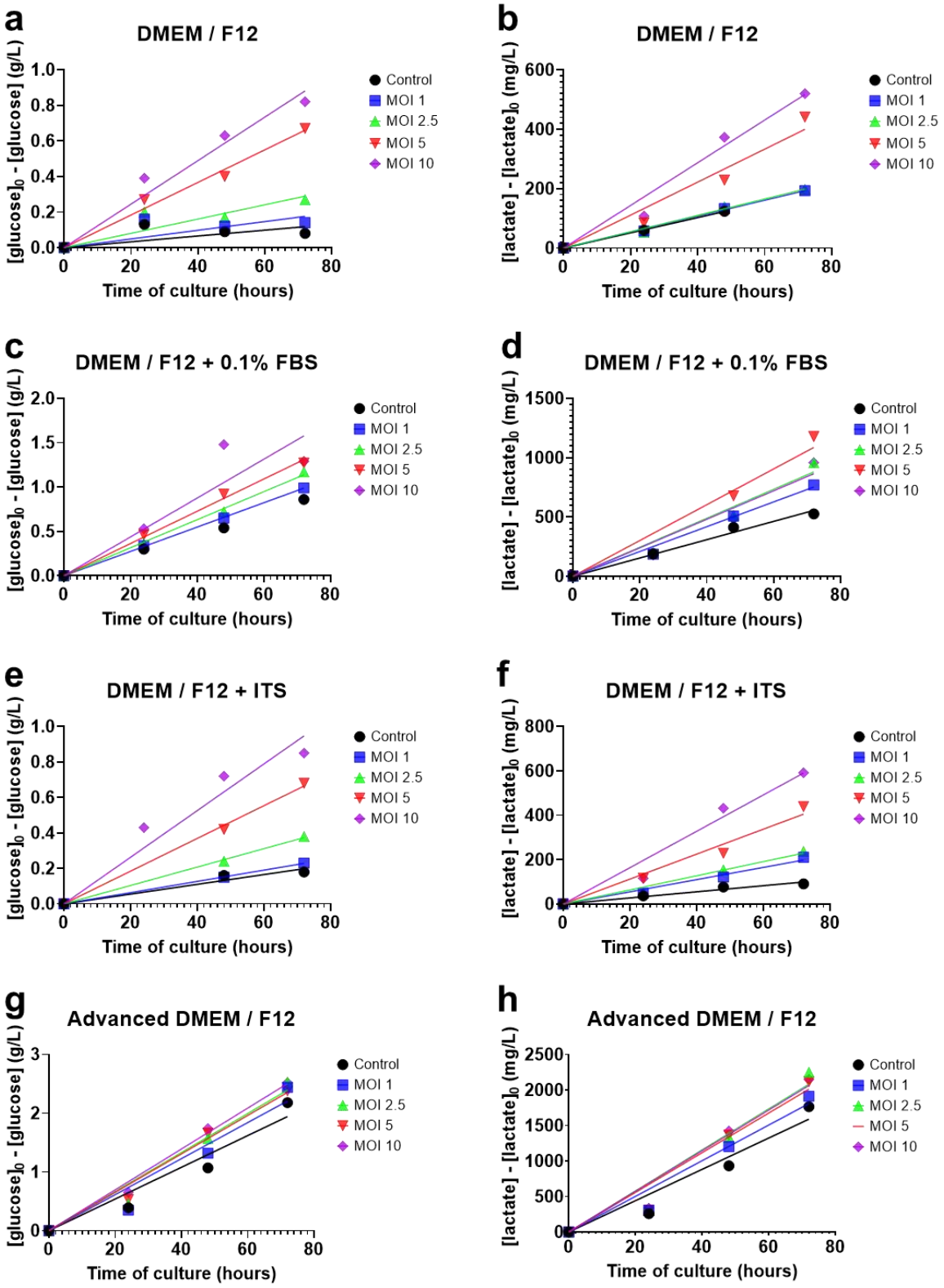


Fig. S1 Volumetric rates of glucose consumption and lactate production in CHO-K1 cell cultures infected with *N. caninum* under different medium conditions. Volumetric rates were calculated from the time-course variations of glucose and lactate concentrations in culture supernatants. For each condition, the rate corresponds to the slope of the line obtained by linear regression of

concentration variation *versus* time data. Panels A, C, E, and G show glucose consumption rates, while panels B, D, F, and H represent lactate production rates. Each row corresponds to a specific culture medium: (A–B) DMEM/F-12, (C–D) DMEM/F-12 + 0.1 % FBS, (E–F) DMEM/F-12 + 1 % ITS, and (G–H) Advanced DMEM/F-12. For each condition, the uninfected control (mock) is shown in black, and infected CHO-K1 cells are represented according to the multiplicity of infection (MOI): 1 (blue), 2.5 (green), 5 (red), and 10 (purple)

Table S2 Volumetric rates of glucose consumption and lactate production in CHO-K1 cultures infected with *N. caninum* under different culture media and multiplicities of infection (MOI). Volumetric rates were calculated from the slopes of linear regression curves obtained from glucose and lactate concentration kinetics over 72 hours of culture. Values are expressed as g/L/h for glucose and mg/L/h for lactate. CHO-K1 cells were cultured in four different media: DMEM/F-12, DMEM/F-12 supplemented with 0.1 % foetal bovine serum (FBS), DMEM/F-12 supplemented with ITS (1 %), and Advanced DMEM/F-12. Infection conditions correspond to multiplicities of infection (MOI) of 1, 2.5, 5, and 10

Medium	Volumetric rates									
	Glucose (g/L/h)					Lactate (mg/L/h)				
	Control	MOI = 1	MOI = 2.5	MOI = 5	MOI = 10	Control	MOI = 1	MOI = 2.5	MOI = 5	MOI = 10
DMEM / F-12	1.64×10^{-3}	2.44×10^{-3}	4.02×10^{-3}	9.71×10^{-3}	11.8×10^{-3}	2.57	2.69	2.76	5.55	7.19
DMEM / F-12 + 0.1 % FBS	11.8×10^{-3}	13.7×10^{-3}	15.8×10^{-3}	18.2×10^{-3}	21.9×10^{-3}	7.72	10.5	12.2	15.1	12.0
DMEM / F-12 + 1 % ITS	2.76×10^{-3}	3.17×10^{-3}	5.19×10^{-3}	9.23×10^{-3}	1.32×10^{-3}	1.38	2.76	3.19	5.63	8.20
Advanced DMEM / F-12	27.0×10^{-3}	30.7×10^{-3}	33.3×10^{-3}	32.7×10^{-3}	34.8×10^{-3}	22.1	25.2	29.0	28.0	28.7

1037 **Table S3** Global rates of glucose consumption and lactate production in CHO-K1 cultures
1038 infected with *N. caninum*. Global rates were obtained by multiplying volumetric rates by the total
1039 culture volume per well (2 mL). Values are expressed in g/h for glucose and mg/h for lactate. CHO-
1040 K1 cells were cultured in DMEM/F-12, DMEM/F-12 + 0.1 % FBS, DMEM/F-12 + ITS, or Advanced
1041 DMEM/F-12 under increasing multiplicities of infection (MOI = 1, 2.5, 5, 10)

1042

Medium	Global rates									
	Glucose (g/h)					Lactate (mg/h)				
	Control	MOI = 1	MOI = 2.5	MOI = 5	MOI = 10	Control	MOI = 1	MOI = 2.5	MOI = 5	MOI = 10
DMEM / F-12	3.27×10^{-6}	4.88×10^{-6}	8.04×10^{-6}	18.3×10^{-6}	23.6×10^{-6}	5.13×10^{-3}	5.38×10^{-3}	5.52×10^{-3}	11.1×10^{-3}	14.4×10^{-3}
DMEM / F-12 + 0.1 % FBS	23.6×10^{-6}	27.4×10^{-6}	31.6×10^{-6}	36.4×10^{-6}	43.8×10^{-6}	15.4×10^{-3}	20.9×10^{-3}	24.5×10^{-3}	30.2×10^{-3}	24.0×10^{-3}
DMEM / F-12 + 1 % ITS	5.51×10^{-6}	6.35×10^{-6}	10.4×10^{-6}	18.5×10^{-6}	26.3×10^{-6}	2.76×10^{-3}	5.51×10^{-3}	6.38×10^{-3}	11.3×10^{-3}	16.4×10^{-3}
Advanced DMEM / F-12	54.0×10^{-6}	61.4×10^{-6}	26.5×10^{-6}	65.4×10^{-6}	69.6×10^{-6}	44.2×10^{-3}	50.3×10^{-3}	57.9×10^{-3}	55.9×10^{-3}	57.4×10^{-3}

1043

1044